(4)

CONTRACT REPORT BRL-CR-606

BRL

EXPLORATORY DEVELOPMENT ON A NEW PROCESS TO PRODUCE IMPROVED RDX CRYSTALS: SUPERCRITICAL FLUID ANTI-SOLVENT RECRYSTALLIZATION

V. J. KRUKONIS
M. P. COFFEY
P. M. GALLAGHER

~~JANUARY 1989~~
May 2, 1988

U.S. ARMY LABORATORY COMMAND

BALLISTIC RESEARCH LABORATORY

ABERDEEN PROVING GROUND, MARYLAND

SECURITY CLASSIFICATION OF THIS PAGE

REPORT DOCUMENTATION PAGE

Form Approved OMB No. 0704-0188

1a. REPORT SECURITY CLASSIFICATION UNCLASSIFIED	1b. RESTRICTIVE MARKINGS
2a. SECURITY CLASSIFICATION AUTHORITY	3. DISTRIBUTION/AVAILABILITY OF REPORT APPROVED FOR PUBLIC RELEASE; DISTRIBUTION UNLIMITED
2b. DECLASSIFICATION/DOWNGRADING SCHEDULE	
4. PERFORMING ORGANIZATION REPORT NUMBER(S) BRL-CR-606	5. MONITORING ORGANIZATION REPORT NUMBER(S)
6a. NAME OF PERFORMING ORGANIZATION Phasex Corporation 6b. OFFICE SYMBOL (If applicable)	7a. NAME OF MONITORING ORGANIZATION Ballistic Research Laboratory
6c. ADDRESS (City, State, and ZIP Code) 360 Merrimack Street Lawrence, MA 01843	7b. ADDRESS (City, State, and ZIP Code) Aberdeen Proving Ground, MD 21005-5066
8a. NAME OF FUNDING/SPONSORING ORGANIZATION Ballistic Research Laboratory 8b. OFFICE SYMBOL (If applicable) SLCBR-TB-EE	9. PROCUREMENT INSTRUMENT IDENTIFICATION NUMBER
8c. ADDRESS (City, State, and ZIP Code) Aberdeen Proving Ground, MD 21005-5066	10. SOURCE OF FUNDING NUMBERS PROGRAM ELEMENT NO. / PROJECT NO. 1L162636D22 / TASK NO. / WORK UNIT ACCESSION NO.

11. TITLE (Include Security Classification)
EXPLORATORY DEVELOPMENT ON A NEW PROCESS TO PRODUCE IMPROVED RDX CRYSTALS: SUPERCRITICAL FLUID ANTI-SOLVENT RECRYSTALLIZATION

12. PERSONAL AUTHOR(S)
Krukonis, V. J.; Coffey, M. P.; Gallagher, P.M.

13a. TYPE OF REPORT	13b. TIME COVERED	14. DATE OF REPORT (Year, Month, Day)	15. PAGE COUNT
Final	FROM Sep 86 TO Jan 88	88/5/2	

16. SUPPLEMENTARY NOTATION

17. COSATI CODES		
FIELD	GROUP	SUB-GROUP
19	01	
19	01	

18. SUBJECT TERMS (Continue on reverse if necessary and identify by block number)
explosives, recrystallization, RDX, supercritical fluids, HMX, fine particals.

19. ABSTRACT (Continue on reverse if necessary and identify by block number)

Topic A86-142 of the FY 1986 DOD SBIR Solicitation sought investigation of methods which could produce improved intragranular cavity-free RDX (cyclotrimethylenetrinitramine) crystals of 100-150 microns size. RDX produced by the current method, recrystallization from cyclohexanone-water solution by evaporative concentration, contains intragranular cavities; they can interfere with the performance of the explosive.

Phasex Corporation proposed the use of supercritical fluids as anti-solvents to recrystallize RDX from organic solvent solution. The concept is based upon the phenomenon of absorption of gas near its critical point by an organic solvent. The absorption of the gas lowers the dissolving power of the organic solvent for RDX resulting in nucleation of RDX. It was suggested that process parameters such as RDX concentration, organic solvent, gas pressure and temperature, rate of introduction of gas and similar factors could be controlled to form the desired particles. Based upon early demonstrations of the supercritical fluid anti-solvent recrystallization capabilities, the main objective of the work viz., the

20. DISTRIBUTION/AVAILABILITY OF ABSTRACT ☒ UNCLASSIFIED/UNLIMITED ☐ SAME AS RPT. ☐ DTIC USERS	21. ABSTRACT SECURITY CLASSIFICATION UNCLASSIFIED
22a. NAME OF RESPONSIBLE INDIVIDUAL WARREN W. HILLSTROM	22b. TELEPHONE (Include Area Code) 301-278-6571 / 22c. OFFICE SYMBOL SLCBR-TB-EE

DD Form 1473, JUN 86 Previous editions are obsolete. SECURITY CLASSIFICATION OF THIS PAGE

19. ABSTRACT cont.

formation of 150 micron RDX crystals free of cavities, was later modified to include the formation of small (20 micron) diameter intragranular cavity-free RDX crystals.

During Phase I, a wide range of parameters was investigated. By the end of the work it was shown that the supercritical fluid anti-solvent process could be controlled to produce RDX crystals of narrow particle size distribution; RDX of 150 microns and RDX crystals of less than 20 micron size were formed from cyclohexanone using carbon dioxide as the anti-solvent. An economic assessment of the process at the 10,000,000 lbs/yr production level showed that RDX could be recrystallized at total capital and operating costs of about $0.50 to $1.00/lb.

TABLE OF CONTENTS

I. SUMMARY

Topic A86-142 of the FY 1986 DOD SBIR Solicitation sought investigation of methods which could produce improved intragranular cavity-free RDX (cyclotrimethylenetrinitramine) crystals of 100-150 microns size. RDX produced by the current method, recrystallization from cyclohexanone-water solution by evaporative concentration, contains intragranular cavities; they can interfere with the performance of the explosive.

Phasex Corporation proposed the use of supercritical fluids as anti-solvents to recrystallize RDX from organic solvent solution. The concept is based upon the phenomenon of absorption of gas near its critical point by an organic solvent. The absorption of the gas lowers the dissolving power of the organic solvent for RDX resulting in nucleation of RDX. It was suggested that process parameters such as RDX concentration, organic solvent, gas pressure and temperature, rate of introduction of gas and similar factors could be controlled to form the desired particles. Based upon early demonstrations of the supercritical fluid anti-solvent recrystallization capabilities, the main objective of the work, viz., the formation of 150 micron RDX crystals free of cavities, was later modified to include the formation of small (<20 micron) diameter intragranular cavity-free RDX crystals.

During Phase I a wide range of parameters was investigated. By the end of the work it was shown that the supercritical fluid anti-solvent process could be controlled to produce RDX crystals of narrow particle size distribution; RDX of 150 microns and RDX crystals of less than 20 micron size were formed from cyclohexanone using carbon dioxide as the anti-solvent. An economic assessment of the process at the 10,000,000 lbs/yr production level showed that RDX could be recrystallized at total capital and operating costs of about $0.50 to $1.00/lb.

II. BACKGROUND ON SUPERCRITICAL FLUIDS

During the late 1970's and early 1980's supercritical fluids were highly touted for their advantages in separating or purifying many materials. Many "misapplications" of supercritical fluids were investigated by research groups all over the world. There was a reversal in interest when the applications to which supercritical fluids were first addressed did not result in industrially attractive separations processes. Therefore, before presenting the results of the RDX recrystallization program a discussion of supercritical fluid solubility phenomena and viable applications is given in order to acquaint the reader with the quite interesting characteristics of these unique solvents. Some of the viable applications developed to a commercial scale, and therefore, supercritical fluid extraction is no longer just a conceptual process or laboratory curiosity that it was considered to be in the early 1980's. Its application to recrystallizing explosives is technically and economically attractive, and it promises to be a viable industrial processing method.

A. Phenomena

The phenomenon of solubility in supercritical fluids was first reported 109 years ago by Hannay and Hogarth[1] who described their observations of the behavior of solid materials dissolved in supercritical fluids. They investigated the solubility of several inorganic salts, e.g., cobalt chloride, potassium iodide, and others, in supercritical ethanol and ether, and their experiments were carried out in a high pressure glass cell so that they could observe the behavior of the solution as conditions of pressure and temperature were varied. The most important result of their experiments was the finding that at conditions above the critical temperature solely a change in pressure caused a change in the solubility of the solid, or stating their finding in a different way, thay observed that solely a change in pressure caused a change in the dissolving power of the solvent.

The pressure dependence of the dissolving power of a supercritical fluid is not limited to inorganic salt solutes, but instead it is general phenomenon exhibited by all supercritical solvent-solid solute solutions and by many supercritical fluid-liquid solute solutions.[2] Many technical papers describing the results of solubility measurements with a number of organic compounds have developed the thermodynamic framework, and the framework allows some reasonably good estimates of the behavior of many other solute-solvent systems to be made.[3-5] In the references cited above, the solubility of naphthalene has been used as the model system for most of the theoretical developments, and the solubility of naphthalene has been the most widely studied experimentally. The solubility behavior of naphthalene in supercritical carbon dioxide is similar to that of other solute-supercritical solvent binary systems, and this large data base can be used to describe the concept of supercritical fluid extraction.

Diepen and Scheffer[6] were the first of many recent workers who studied the phase behavior of naphthalene in ethylene at high pressure, and this paper was followed with more studies from the two authors and their co-workers[7,8,9,10]. Of historical interest here, Buchner first studied the

solubility behavior of naphthalene in carbon dioxide in 1905[11]; an interesting summary of the early (and controversial) period of supercritical fluid solubility study is given in Reference 2. Other workers who examined the solubility and phase behavior of naphthalene were Tsekhanskaya, et al[12,13,14], King and Robertson[15], Najour and King[16], MacKay and Paulaitis[8], McHugh and Paulaitis[9], Kurnik and Reid[10], Schmitt and Reid[17], Krukonis, et al[18], McHugh, et al[19]. The solubility and phase behavior of naphthalene have been studied in methane, ethylene, ethane, carbon dioxide, chlorotrifluoromethane, and trifluoromethane and the last two groups[18,19] extended the studies of naphthalene solubility using xenon as the solvent. Thus, as was stated earlier, there exists a great deal of information about the solubility of naphthalene in a number of gases. Many other solids besides naphthalene have been studied for their behavior in supercritical fluid solvents, e.g., biphenyl[9], eicosane[20], anthracene[21], phenanthrene[22], benzoic acid[23], and still many others[24,25,26,27].

As an example of the pressure dependent dissolving power of a supercritical fluid, Figure 1 gives data on the solubility of naphthalene in carbon dioxide at 45°C[13]. As the figure shows, the solubility of naphthalene in carbon dioxide is very small at low pressure, which is not unexpected since low pressure gases are not good solvents, but as the critical pressure of carbon dioxide (71 atm) is approached, the solubility of naphthalene starts to increase; it increases very rapidly as the pressure is raised above the critical pressure. The solubility values (which were given in units of g/l in the referenced paper) approach about 10% (w/w) at pressure levels of 200 atm. Figure 2 assembles a large amount of data on naphthalene solubility from the previously referenced works[28]. The curves shown in the figure give the isobaric solubility values of naphthalene in carbon dioxide as a function of temperature (and the dotted line shows the solubility of naphthalene in saturated liquid and in saturated vapor).

As related earlier, all solid compounds (and many liquids) exhibit similar solubility behavior in supercritical fluids. To provide partial corroboration for the statement the solubility behavior of another system, silica-water, is shown in Figure 3. The pressure and temperature levels are quite different from those of naphthalene-carbon dioxide shown in Figure 2, (because the critical temperature and pressure of the two solvents are different), but the overall appearance of the isobars is very similar in appearance. For one more example, the solubility behavior of triglycerides (e.g., soy bean oil) in carbon dioxide is given in Figure 4. The similarity of all the figures is evident.

B. Extraction Process Operation

Because of the solubility characteristics shown in Figures 1-4, it is possible to design industrial processes to extract, purify, and/or fractionate materials based upon changes in pressure on a supercritical fluid solvent; at high pressure an extraction can be effected, and lowering the pressure elsewhere in the process causes the dissolved material to separate from the solvent which can then be recycled to the extractor. The process can be operated as either a batch or a continuous one depending upon the nature of the feed and the nature of the extraction, i.e., whether it be a purification

FIGURE 1

SOLUBILITY OF ORGANICS IN SUPERCRITICAL FLUIDS

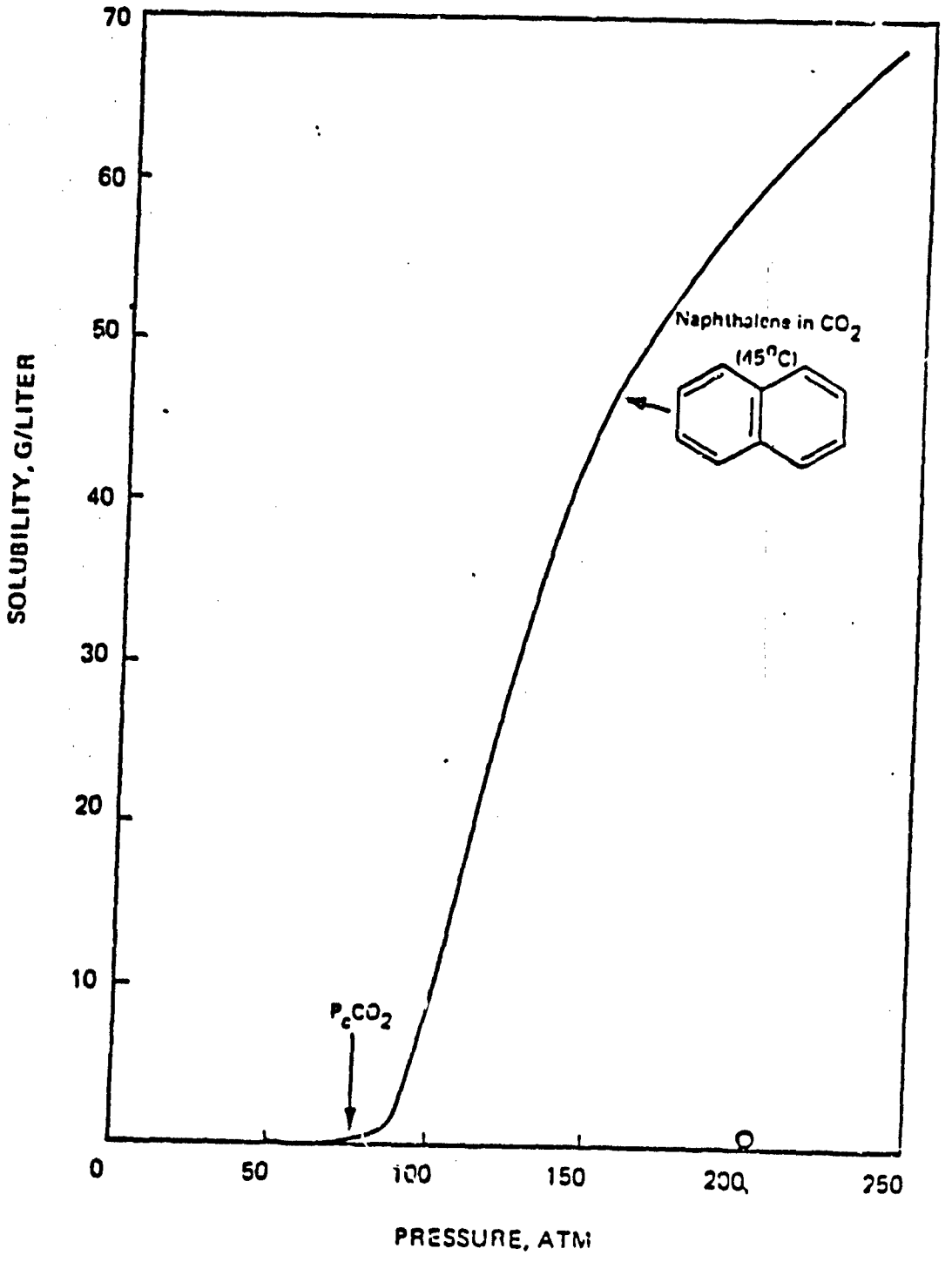

FIGURE 2 -- SOLUBILITY OF NAPHTHALENE IN CARBON DIOXIDE

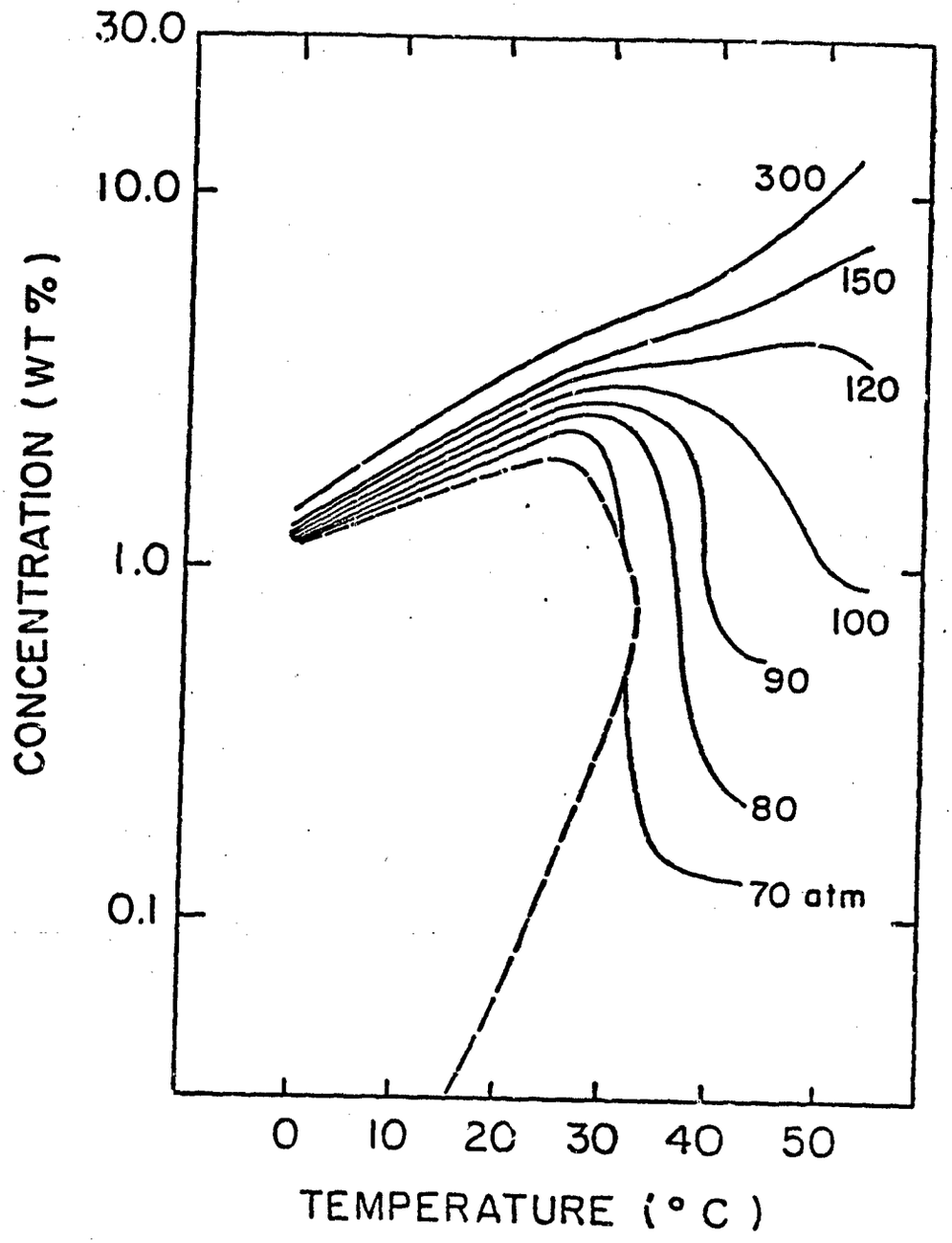

FIGURE 3

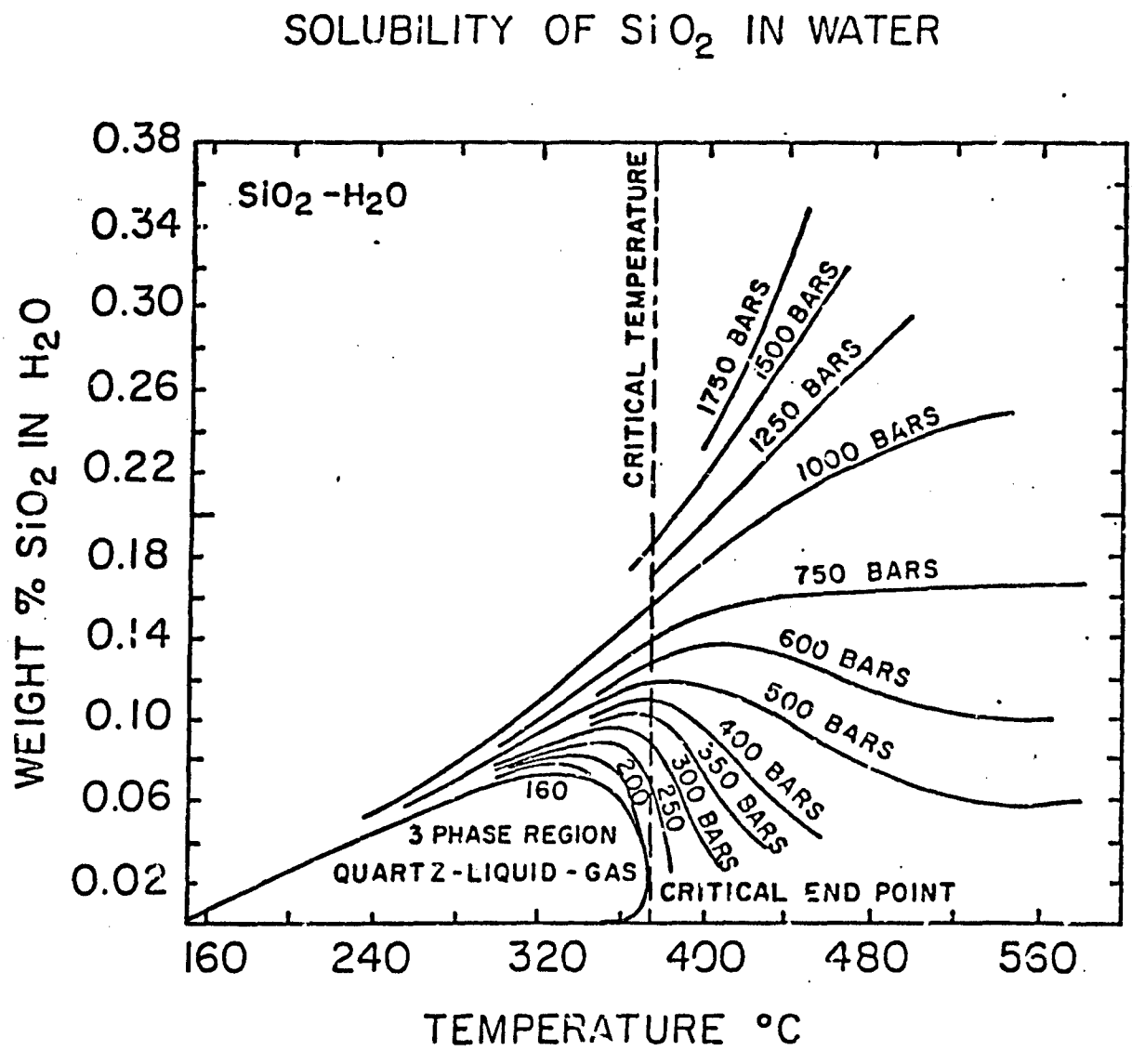
SOLUBILITY OF SiO_2 IN WATER
$SiO_2 - H_2O$
CRITICAL TEMPERATURE
1750 BARS
1500 BARS
1250 BARS
1000 BARS
750 BARS
600 BARS
500 BARS
400 BARS
350 BARS
300 BARS
250
200
160
3 PHASE REGION
QUARTZ - LIQUID - GAS
CRITICAL END POINT
WEIGHT % SiO_2 IN H_2O
0.38
0.34
0.30
0.26
0.22
0.18
0.14
0.10
0.06
0.02
160
240
320
400
480
560
TEMPERATURE °C

FIGURE 4 - SOLUBILITY OF TRIGLYCERIDES IN CARBON DIOXIDE

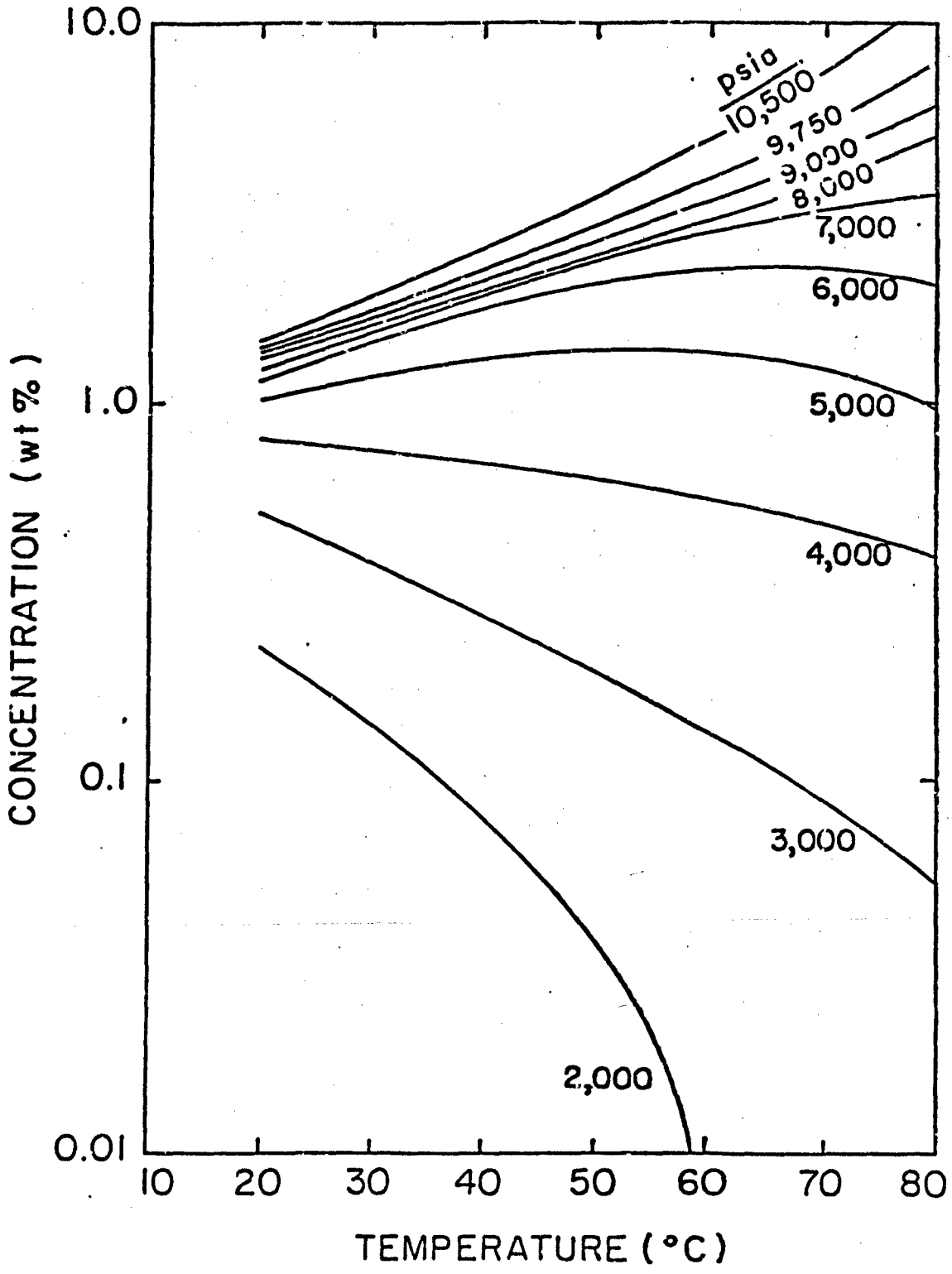

(or topping), a fractionation, or an extraction from a reaction mass. The use of a supercritical fluid solvent in separating materials was first described in the literature by Todd and Elgin in 1955[29]; their phase equilibrium studies of a large number of solutes with supercritical ethylene led them to suggest that industrial separations processes could be readily devised based upon the pressure dependence of solubility.

A schematic diagram of a process which uses a supercritical fluid as a pressure dependent solvent to extract an organic substance is given in Figure 5a. Four basic elements of the process are shown, viz., an extraction vessel, a pressure reduction valve, a separator for collecting the materials that were dissolved in the extractor, and a compressor for recompressing and recycling fluid. (Ancillary pumps, valving, facilities for fluid make-up, heat exchangers, and other equipment are omitted from the figure for clarity and ease of presentation.) Figure 5b shows the extensive data on the solubility of naphthalene in carbon dioxide previously given in Figure 2, and reference to Figures 5a and 5b is made to explain how the supercritical fluid process operates.

Some process operating parameters are indicated on two solubility isobars in Figure 5b; E_1 represents conditions in the extractor, e.g., 300 atm, 55°C, and S_1 the conditions which exist in the separator, 90 atm, 36°C. The extractor vessel is assumed to be filled with naphthalene in admixture with another material that, for this discussion, is assumed to be insoluble in carbon dioxide. Carbon dioxide at conditions E_1 is passed through the extraction vessel wherein it dissolves (and extracts) the naphthalene from the insoluble material. The carbon dioxide-naphthalene solution leaving the extractor is next expanded to 90 atm through the pressure reduction valve and as indicated by the directed path in Figure 5b. During the pressure reduction step, naphthalene precipitates from the solution. (A temperature decrease of about 19°C occurs during the expansion of the stream, and thus, the pressure reduction path shown in Figure 5b is an oblique one.) The naphthalene that nucleates and precipitates when the pressure is reduced is collected in the separator, and the carbon dioxide leaving the separator is recompressed and returned to the extractor. This recycle process continues until all the naphthalene is dissolved and extracted, the directed line segment 1 - 2 and its reverse on the solubility diagram representing approximately the cyclic process.

As an alternative to extraction and separation using pressure reduction (i.e., the path 1 - 2) the process can operate at constant pressure and temperature changes in a supercritical fluid can be used to effect the extraction and separation steps. For example, and again starting at 1, the stream leaving the extractor could be passed through a heat exchanger (instead of a pressure reduction valve) and cooled to, say, 20°C as indicated by the directed portion on the 300 atm isobar. Cooling the stream would result in the precipitation and collection of naphthalene in the separator at conditions 3. The carbon dioxide leaving the separator could then be passed through another heat exchanger located downstream of the separator and heated back to 55°C before being recycled to the extractor. A fluid recirculating pump is still required, but it would supply pressure only for frictional and momentum losses; these are small.

FIGURE 5a - EXTRACTION PROCESS

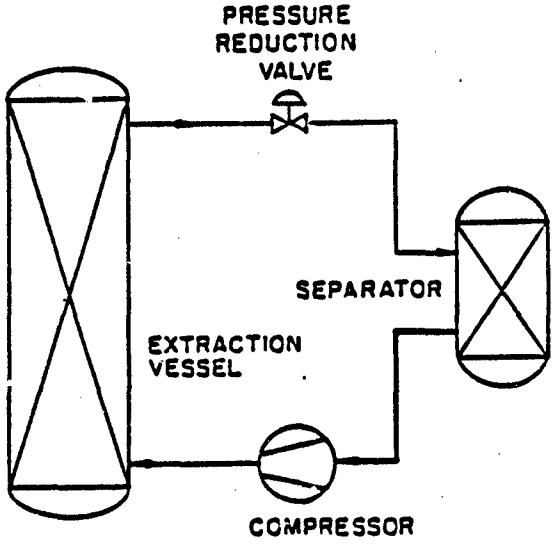

FIGURE 5b - OPERATING CONDITIONS

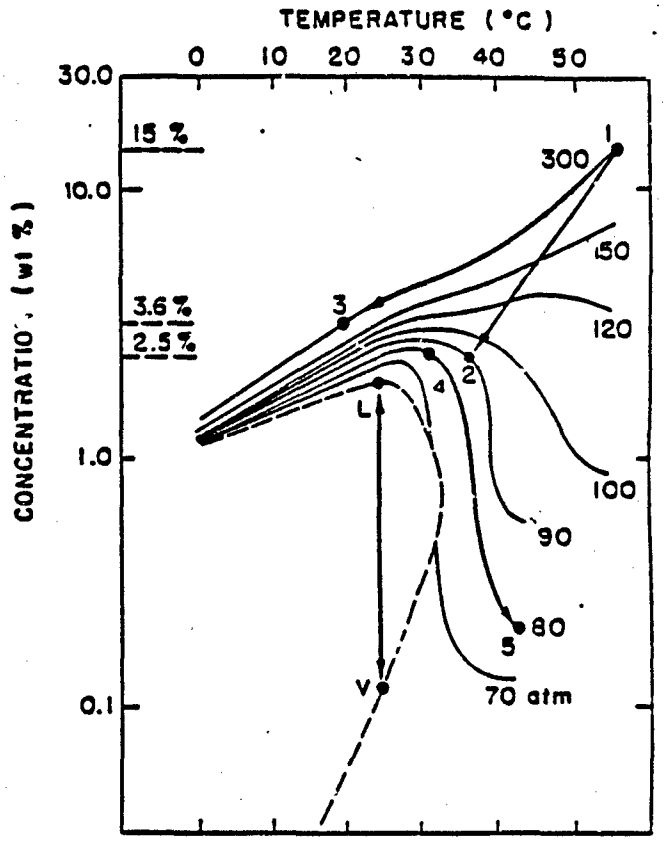

There are regions where the solubility decreases with increasing temperature, a behavior not usually exhibited by liquid solvents at room temperature and advantages of this behavior can also be made in carrying out an extraction and separation. For example, the extraction of naphthalene could be carried out at, say, 30°C and 80 atm starting at point 4 and a 10-fold change in solvent dissolving power could be caused by heating the solution only about 10°C to 40°C; the naphthalene that precipitates would be collected, as before, in the separator. Cooling the carbon dioxide back to 30°C would raise its solvent power and it could be recycled for further extraction. In another variation, carbon dioxide can be employed like "normal" liquid solvents. As stated earlier, the dashed curve shows the solubility of naphthalene in liquid and in vapor carbon dioxide. Thus, liquid carbon dioxide at point L can be used to extract naphthalene from the mixture and elsewhere in the process the carbon dioxide can be vaporized; the naphthalene would precipitate in the vaporizer since the vapor at point V contains negligible naphthalene. To complete the cycle, the vapor is condensed and returned to the extractor. Which specific process to use in any particular extraction is based upon an evaluation of many factors. The case chosen for discussion, i.e., naphthalene extraction from another insoluble material, is an idealized one. In an actual case there may be many materials in the mixture that exhibit varying degrees of solubility. Determining an optimum balance of gas requirements, yield, selectivity, and other factors is determined on a case-by-case basis.

It has been expedient to use the naphthalene data to present the concept of the pressure-dependent solvation power of supercritical fluids, but the process concept shown in Figure 5 is quite general, applying to any material that exhibits the solubility behavior shown in Figures 2-4.

C. Process Applications of Supercritical Fluid Extraction

A large number of applications has been studied in the laboratory during the last ten years; some have progressed to the industrial scale and as an illustration of the many kinds of materials that can be treated by supercritical fluids a partial list of some of these applications is given in Table I.

Table I

SUPERCRITICAL FLUID APPLICATIONS TESTED

Extraction of Spices, Natural Colorants, Essential Oils,[30,31,32]

Separation of Ethanol-Water[33,34,35,36]

Regeneration of Activated Carbon[37,38]

Extraction of Caffeine from Coffee, Tea[39,40,41,42]

Extraction of Oil from Soy Beans[43,44,45]

Extraction of Vegetable Oil from Potato Chips[46]

Energy Related Extractions; Coal, Residuum, Oil Shale[47,48,49]

Extraction of Chemotherapeutic Drugs from Plant Materials[50,51]

Extraction of Naval Stores from Wood Chips[52]

The fact that supercritical extraction "works" in the applications listed above does not necessarily mean that the processes will be viable industrially. For example, during the late 1970's much effort was directed to the development of a supercritical fluid extraction process for separating ethanol from water[53]. It was suggested that because carbon dioxide could extract ethanol from water with less energy than is required in a distillation process, supercritical fluid separation would be economically viable. All facets of a process must be considered, however, not just the energy costs, and in the case of alcohol-water separation, the higher capital cost for the equipment outweighed the cost savings of reduced energy requirements, and the process was found to be not economically viable. On the other hand hops extraction using supercritical carbon dioxide is commercial in the U.S., and a large plant is being operated by Pfizer Inc. in Sidney, NE[54]. Additionally, General Foods has constructed a coffee decaffeination plant in Houston, TX that is scheduled for start up in the spring of 1988[55]. The added value to the improved products that derive from supercritical extraction more than compensates for the cost of extraction relative to conventional solvent extraction, for example, with methylene chloride. In West Germany, there are three large supercritical fluid extraction plants in operation, one decaffeinating coffee at a production rate of 60,000,000 lbs/yr[56], and two plants extracting hops.

During the past five years many "newer" applications of supercritical fluid extraction have been examined; examples of such operations are reactive monomer purification and polymer fractionation[57,58,59], two areas where the properties of supercritical fluids can be technically and economically attractive. Additionally, recrystallization of materials dissolved in supercritical fluids was first suggested by Phasex Corporation in 1981[60a], but actually the concept is based upon the principles first discovered by Hannay and Hogarth[1] who were referenced earlier. It is of interest to quote from the closing statements of their 1879 publication,

> "We have, then, the phenomenon of a solid with no measurable vapor pressure, dissolving in a gas ..."
>
> "When the solid is precipitated by suddenly reducing the pressure, ... it may be brought down as a 'snow' in the gas ..."

Thus, the supercritical fluid extraction process that was described previously in Section II can be operated so as to produce recrystallized materials. For example, the naphthalene that was precipitated after it was dissolved and extracted in the process shown in Figure 5 would assuredly be of different particle size than the naphthalene in the original mixture. Thus, any soluble solid material can be charged to an extraction vessel, dissolved in a supercritical fluid, the solution expanded to some lower pressure level and the particles formed collected in a separator. Some results of using the supercritical fluid nucleation concept were reported in 1983[60b] and 1984[60c]; examples of nucleating a wide variety of materials such as steroids, dyes, and polymers were presented. Figure 6, for example, compares as received and supercritical fluid nucleated particles of an estrogen; the recrystallized particles are seen to be quite uniform and of the order of one micron in size, whereas the control (as received) material exhibits a quite wide particle size

FIGURE 6

Photomicrographs:
(a) virgin particles of β-estradiol; (b) particles of β-estradiol nucleated from an SCF solution

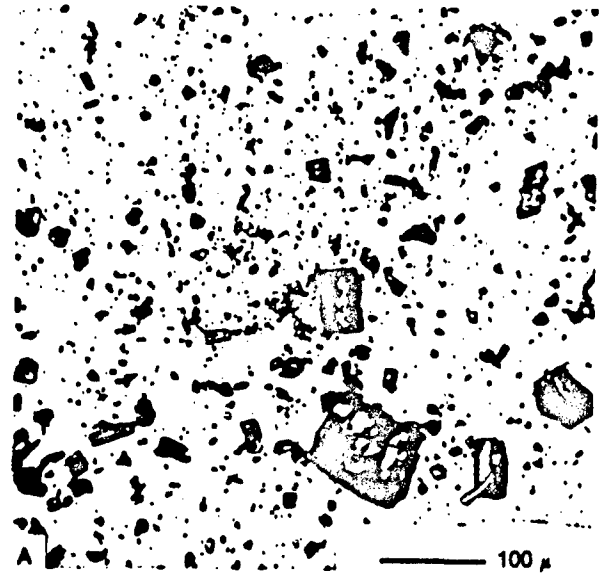

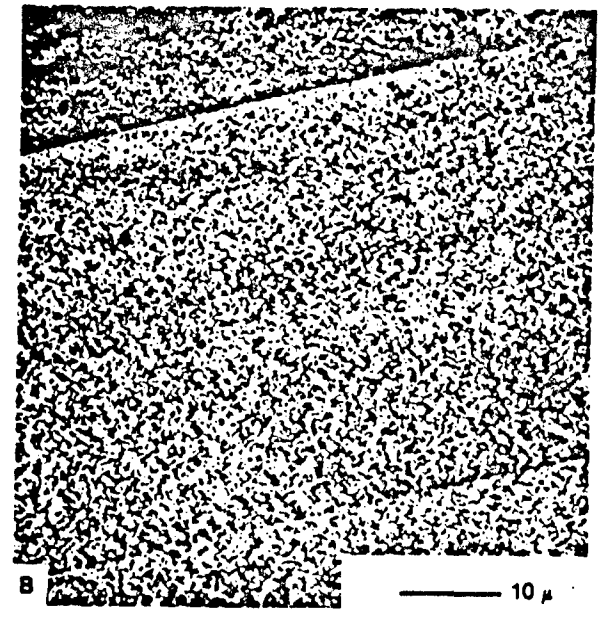

distribution with many large particles present. Other groups later reported on supercritical fluid nucleation of pharmaceuticals[61] and polymers[62].

For the nucleation process to work as described above, the solid material must, of course, exhibit some level of solubility in the supercritical fluid; the "snow" described by Hannay and Hogarth is formed when a solution of the solute and supercritical fluid is expanded to a lower pressure.

If a material does not dissolve in a supercritical fluid, the concept as described cannot be employed. RDX does not dissolve in any of the "simple" gases, e.g., carbon dioxide and the light hydrocarbons, methane, ethane, ethylene, and the chlorofluorocarbons, yet a supercritical fluid can still be used as a nucleating solvent for RDX. The principle of precipitation in this case is different, however, but there are no limitations to the use of the process for any material provided that certain solubility relationships exist among the material, the organic solvent, and the supercritical fluid. The next section explains the principle of gas anti-solvent nucleation in those cases where the solute does not dissolve in a supercritical fluid, and the results obtained on the Phase I program are presented.

III. RDX RECRYSTALLIZATION WITH SUPERCRITICAL FLUID ANTI-SOLVENTS

A. Principle of Supercritical Fluid Anti-Solvent Precipitation

The most widely known supercritical fluid nucleation process was described in the previous section, the requirement for that concept to be operable being that the solid material dissolve in the fluid. If the compound does not dissolve in the supercritical fluid, a supercritical fluid can nonetheless be employed in a process to recrystallize the material, viz., it can act as an anti-solvent the general requirement being that the material to be crystallized dissolve in some organic solvent and that the fluid also dissolve in that solvent.

Results using supercritical fluids to separate solutions of liquids were first reported in 1959 by Elgin and Weinstock[63]. The researchers showed that solutions of water and an organic solvent could be separated into a water-rich phase and an organic-rich phase with supercritical ethylene, and they termed the process "supercritical fluid salting out". The salting out process is quite generally applicable to water-organic solvent solutions if the supercritical fluid is miscible with the organic liquid, if the concentration of organic liquid in the solution is "high" (with "high" a function of the specific organic liquid), and if the intermolecular forces between water and the organic are not "too great". For example, the workers showed that a solution of water-methyl ethyl ketone (MEK) can be split into a water-rich phase and an organic-rich phase by the action of supercritical ethylene. In explanation of the process of separation, the supercritical fluid, ethylene, which is miscible with neat MEK, will dissolve in the water-MEK solution; when sufficient ethylene has dissolved, it will act as an anti-solvent for water, and two phases will be formed.

More recently Paulaitis, et al[64] report on the phase equilibria of isopropanol water-carbon dioxide solutions, and it is instructive to reproduce their data here as an aid in explaining the events that occur when carbon dioxide is introduced into a solution of, say, 50/50 (mol %) isopropanol-water. Figure 7 shows the ternary diagram for isopropanol-water-carbon dioxide (at conditions of 136 atm and 60°C). "Starting" at the 20% IPA/80% H_2O concentration point (point 1), if carbon dioxide is introduced (depicted by the directed dotted line) and mixed to equilibrium with the solution, the carbon dioxide will dissolve into the solution. When "sufficient" carbon dioxide has been dissolved, the miscibility characteristics of isopropanol and water will be modified and a second phase will appear (point 2); the amount of the two phases and the concentrations in each phase will be governed by thermodynamic equilibrium considerations for the three components at the conditions of temperature and pressure. The specific concentrations of the phases can be obtained from knowledge of the "tie lines", i.e., the concentrations of the two equilibrium phases at any combination of components, temperature, and pressure, and the amounts of each phase can be obtained from the "lever rule", the material balance relating the "unmixed" composition to the composition of the equilibrium phases. For example, if enough carbon dioxide is added to the solution to reach point 3, the two equilibrium phases will have concentrations of 55% IPA (45% H_2O) for the isopropanol-rich (carbon

FIGURE 7

Measured Equilibrium Tie Lines for Isopropanol-Water-CO_2

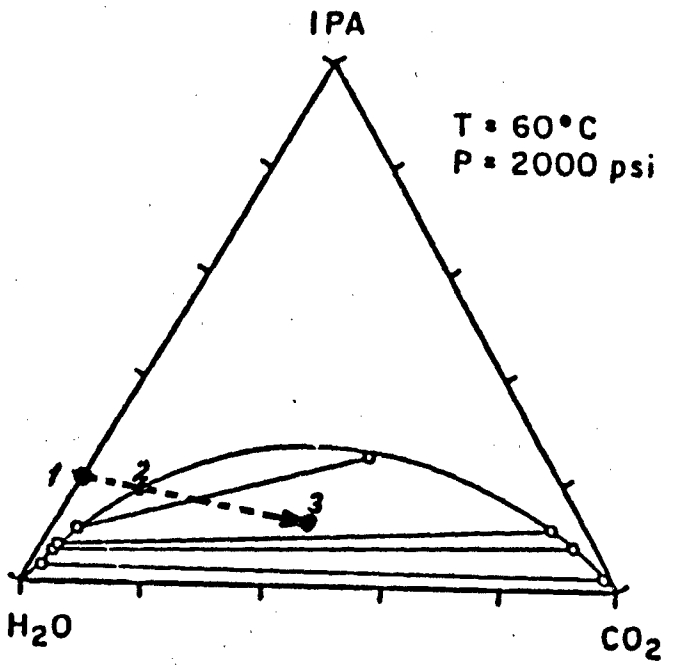

dioxide free basis) phase, and 10% IPA (90% H_2O) for the water-rich phase. These concentrations are determined by the tie line drawn through point 3 intersecting the two-phase envelope at the equilibrium concentrations.

A similar concept was later applied to the separation of polymer-organic solvent solutions, by Irani et al[65] and McHugh, et al[66] who showed that the lower critical solution temperature (LCST) of the polymer solution could be lowered dramatically by the injection of a supercritical fluid. They showed that the separation process could, thus, be carried out at quite modest temperature which can reduce the overall energy requirements and additionally can reduce thermal degradation of the polymer. The explanation for polymer precipitation from organic liquid solution is similar to that for the separation of water from the organic solvent discussed earlier. The organic liquid is a good solvent for the polymer, and the supercritical fluid, say, carbon dioxide again, is not. The carbon dioxide dissolves in the solution, the solution expands to the point whereat the carbon dioxide-organic phase is no longer a solvent for the polymer, and the polymer precipitates. In addition to solubility effects, such considerations as the molecular weight and molecular weight distribution, and polymer composition, influence the extent of precipitation and recovery of polymer from solution.

Polymers can be separated from solution by solely thermal means, and an understanding of the thermal separation concept can be obtained from a phase diagram for a "general" polymer-organic solvent solution. Figure 8 shows a part of a P-T (pressure-temperature) projection of a three dimensional (pressure-temperature-concentration) diagram; this is a two component phase diagram, viz., polymer and organic solvent with no supercritical fluid component present. (In actuality Figure 8 is a "pseudo-two" component diagram because a polymer usually consists of a quite wide range of oligomers which, although they are all homologous series members, influence the thermodynamic characteristics of the system somewhat.) The designation L connotes a single liquid phase region, LL a two liquid phase region, and LLV two liquids and a vapor region. The L region is where the solvent and polymer are miscible.

The diagram points out that one method of separating a polymer from its solution is by raising the temperature of the solution isobarically (as depicted by the Path 1 -- 2); the solution separates into two phases which can be separated, in a decanter for example. As will be discussed later, the temperature levels in the region of the LCST line are usually quite high, and thus crossing the LCST line by raising the temperature as depicted by Path (?) 1 - 2 may not be a viable method industrially if the polymer can degrade at high temperature. (Incidentally, the two phase region in Figure 8, designated LL, consists of two liquid phases rather than a liquid and a solid polymer (LS) because the temperature levels are frequently near or above the softening or melting point of the polymer. Additionally, even if the temperature is below the softening point there still might be two liquid phases in equilibrium because noncrystalline polymers can be swelled and plasticized by solvents, i.e., the solvent can dissolve in the polymer.)

The physical explanation for the split separation of polymer when the solution is heated resides in thermal expansivity considerations. If a liquid is heated to near its critical temperature it expands considerably, and

FIGURE 8

PHASE DIAGRAM (P-T PROJECTION) OF POLYMER - ORGANIC SOLVENT SYSTEM

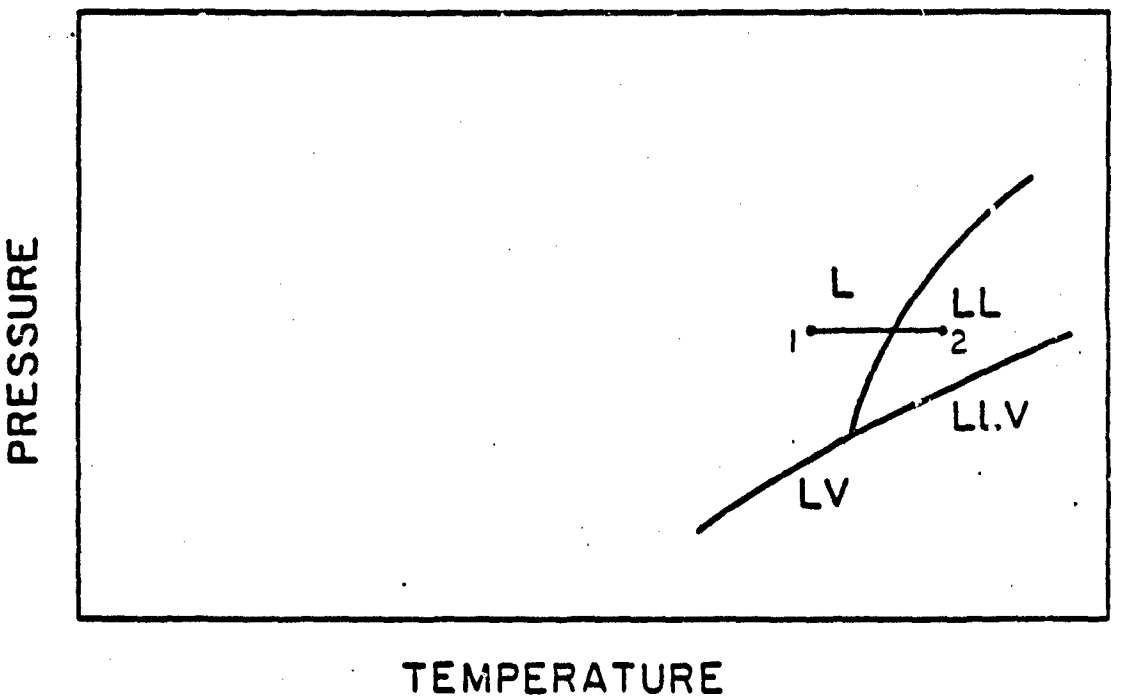

its ability to dissolve polymers (and other substances) is decreased markedly. Thus if a solution containing dissolved polymer at a high concentration is heated, part (and often a substantial amount) of the polymer will precipitate. Unfortunately, as was said above, the critical temperature of a "good" polymer solvent is usually quite high, e.g., 200-300°C, and thus thermal degradation can ensue with some polymers and, furthermore, from an industrial processing standpoint the energy requirements for carrying out the separation can be quite high.

The LCST line and thus separation of polymer from solution can be shifted to much lower temperatures by the expedient of dissolving a supercritical fluid in the polymer-solvent mixture; for example, McHugh et al report that dissolving ethylene in a system composed of hexane-polyethylene co-polypropylene can shift the LCST curve to a regime of much lower temperature. Figure 9 (from Reference 66) shows this. The three P-T projections in Figure 9 show the repositioning of the LCST line toward decreasing temperature with increasing ethylene concentration. A change of 50°C occurs with an ethylene loading change of only 10.1 wt%, from 9.9 to 20 wt%. Incidentally, the position of the LCST line with solely hexane is off scale in Figure 9, 100+°C higher than the 20% line. Thus, the precipitation temperature can be reduced markedly with the use of a supercritical fluid, and thus is especially advantageous for heat sensitive polymers.

The same phenomenon, viz., the addition of a supercritical fluid to a solution of a crystalline solid and an organic solvent, is applicable to separating/recrystallizing a solid explosive providing that the explosive is not "too" soluble in the supercritical fluid. Considering now RDX specifically, if a saturated, or partially saturated, solution of RDX (in cyclohexanone, for example) is contacted with a supercritical fluid, the fluid will dissolve in the solution, will lower the dissolving power of the cyclohexanone for the RDX, and the RDX will nucleate and crystallize. The resultant particle size and size distribution will be a function of many parameters which are explained in this section.

In many respects the supercritical fluid anti-solvent process is analogous to any liquid anti-solvent process that operates industrially. For example, production of Class 5 (25 micron particle size) RDX is one such industrial process. In its operation an acetone solution of RDX is admixed with an anti-solvent, water, which results in precipitation of RDX. The resultant mixture of particles and liquid is filtered to separate the particles of RDX, and the water-acetone filtrate is separated by distillation to recover the acetone for reuse. Another solvent, cyclohexanone, is also used in the RDX manufacturing process, specifically in the production of Class 1 RDX (100-150 microns). In the recrystallization step a solution of RDX in cyclohexanone-water which has been seeded with RDX crystals is heated to evaporate the liquid; with "proper" agitation RDX nucleates and grows on the seed crystals, the specific combination of such parameters as agitation, surfactant, and evaporation rate resulting in the formation of the desired 100-150 micron particles. The evaporated liquid (and water) is subsequently separated by distillation, and the cyclohexanone is recycled.

In the process where a supercritical fluid would be used as the

FIGURE 9

PHASE DIAGRAM (P-T PROJECTION) OF POLYMER - HEXANE - SUPERCRITICAL ETHYLENE SYSTEM

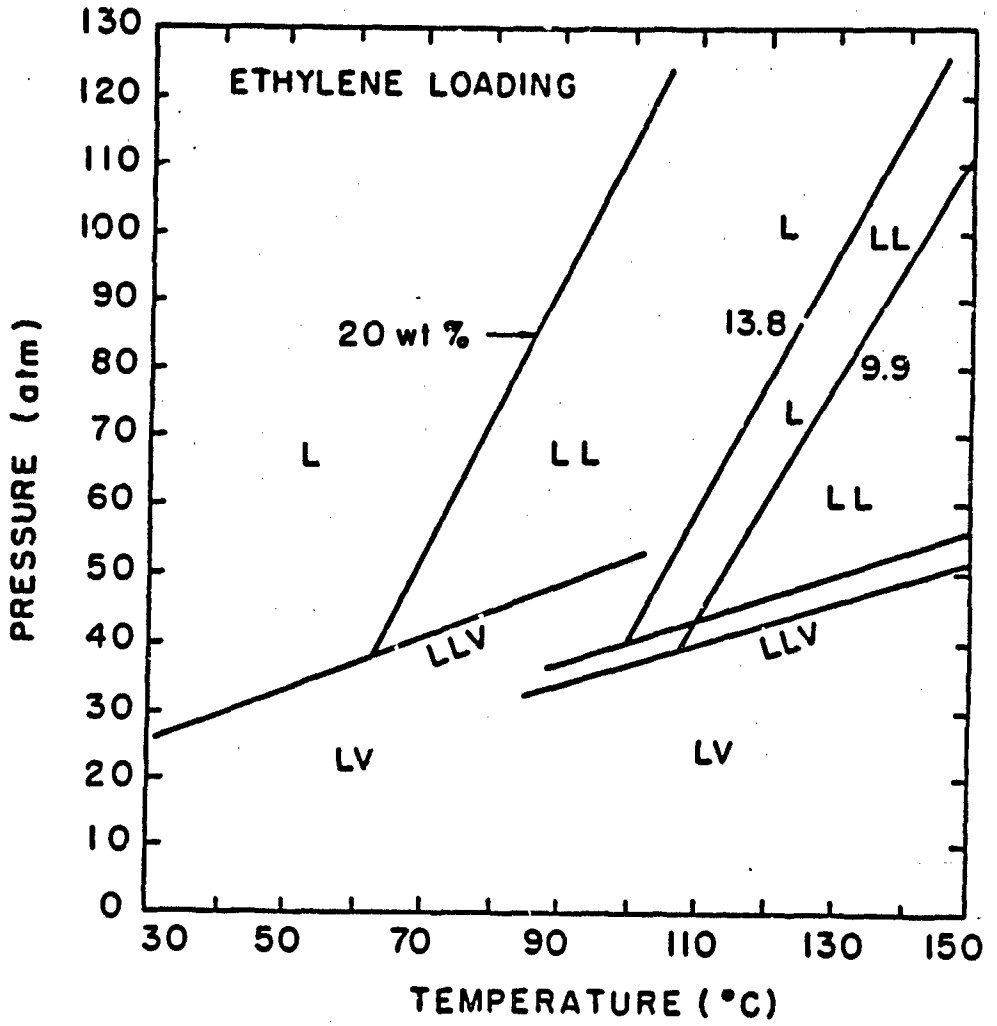

anti-solvent, no distillation step is required. The supercritical fluid-organic solvent solution that leaves the filter can be separated into its components by a simple pressure decrease which causes the gas to be released from solution, and both the gas and the liquid solvent can be re-used. The choice of which process to use where is, like for any industrial process, governed by many factors some of which were addressed in Section II; there are many advantages of supercritical fluid anti-solvent precipitation of RDX, and they are developed after the results of the laboratory program are presented. Briefly, here, the separation of solvent and anti-solvent can be made with quite low energy requirements, and it is discussed subsequently that the recrystallization period can be reduced to a duration of literally minutes or seconds. Additionally it is speculated later that the process can be modified so as to be able to coat the recrystallized explosive with polymers (or other materials) so that they can be stabilized against hydrolytic attack and incorporated into a polymer matrix with ease.

B. Experimental Methodology

In outline of the experimental program that was carried out, acetone and cyclohexanone were used as organic solvents for RDX, and combinations of pressure and temperature, and other supercritical fluid parameters that would recrystallize RDX from the organic solution were tested. Other parameters such as the rate of introduction of the fluid into solution and initial RDX concentration were also considered to be possible influences on the particle size, shape, and particle size distribution of recrystallized RDX and were studied. The supercritical fluids tested were carbon dioxide, ethylene, and ethane.

Two experimental systems were used in the studies, one a sight glass assembly which allows the recrystallization process to be observed, and the other a closed vessel assembly. A schematic diagram of the sight glass assembly, a standard 5000 psi "Jerguson gauge" (Jerguson Gage and Valve Company), is shown in Figure 10a; a photograph of the assembly is shown in Figure 10b. The photograph is centered primarily on the windowed cavity of the sight glass, but the schematic diagram shows all the features for carrying out and observing a recrystallization test and collecting sample for subsequent examination. A thermocouple is positioned in the solution to measure the temperature, it is part of a temperature control circuit not shown in Figure 10a or 10b. A pressure gauge for measuring pressure is positioned at the top of the assembly. The various valves shown permit gas to be introduced, liquid to be drained, and/or gas to be removed from the solution. The cotton plug at the bottom of the cavity serves as a filter for the collection of particles of RDX when the expanded liquid is drained. Precautions were taken to avoid direct contact of sharp metal surfaces with the RDX crystals.

In explanation of the conduct of a recrystallization experiment, an amount of RDX-cyclohexanone solution is charged to the sight glass and the system sealed. Carbon dioxide is admitted at the bottom, and the bubbles of gas entering the cavity both mix the liquid and dissolve in it. As was explained earlier, as the pressure is raised, the carbon dioxide increasingly dissolves in the RDX-cyclohexanone solution, and the solution expands. At "some" pressure level enough dissolution of gas and concomitant expansion has occurred to decrease the dissolving power of cyclohexanone for RDX, at this point crystals begin to nucleate and grow. (A linear motion mixer had been planned for use for the recrystallization studies but because of the knife-edge metal surfaces of the agitator (which could initiate decomposition of RDX), it was not used during the recrystallization tests. During the neat solvent expansion tests the mixer was used and the results of the expansion-pressure experiments were found to be about the same whether the mixer was energized or not, indicating that the agitation caused by the bubbles of supercritical fluid passing through the solvent provided reasonably extensive mixing action and that there was little or no resistance to dissolution of the gas.)

It is difficult to predict a priori the particle size, and shape, and particle size distribution that will result from some specific combinations of

Figure 10a Schematic Diagram of Sight Glass

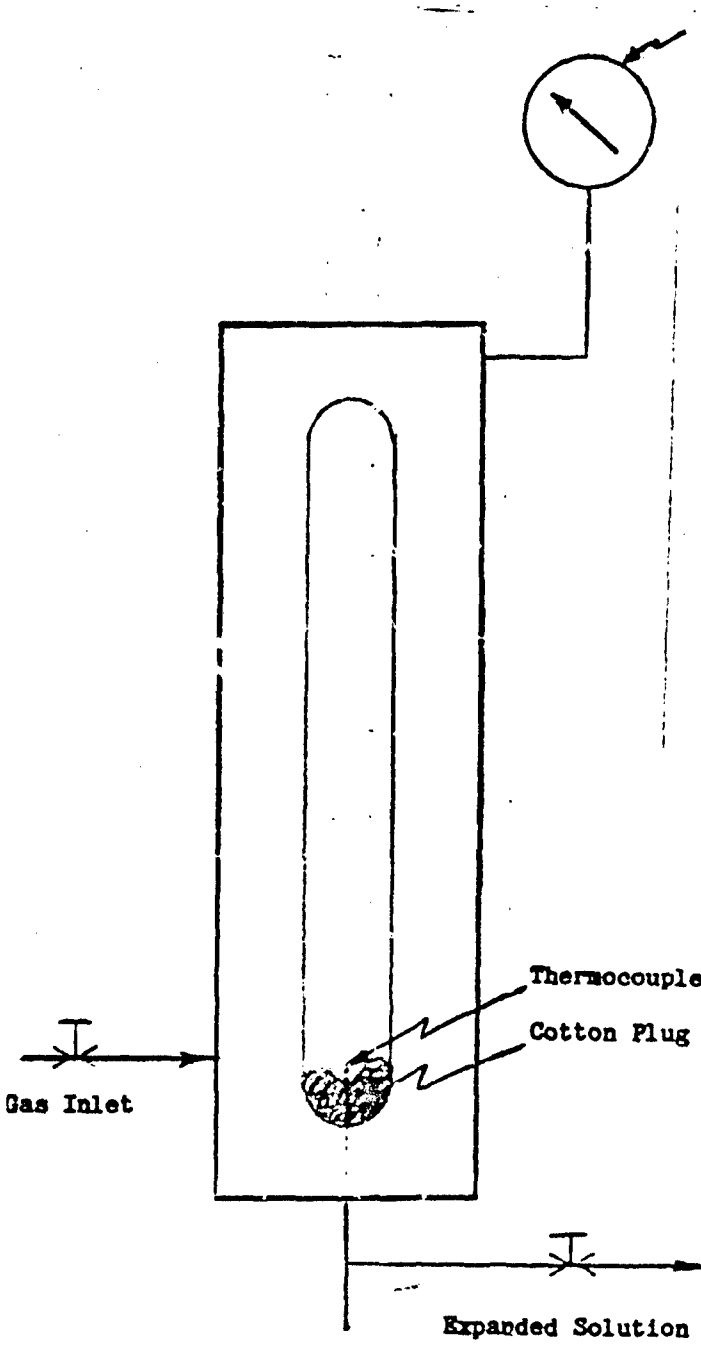

Figure 10b Photograph of Sight Glass Assembl

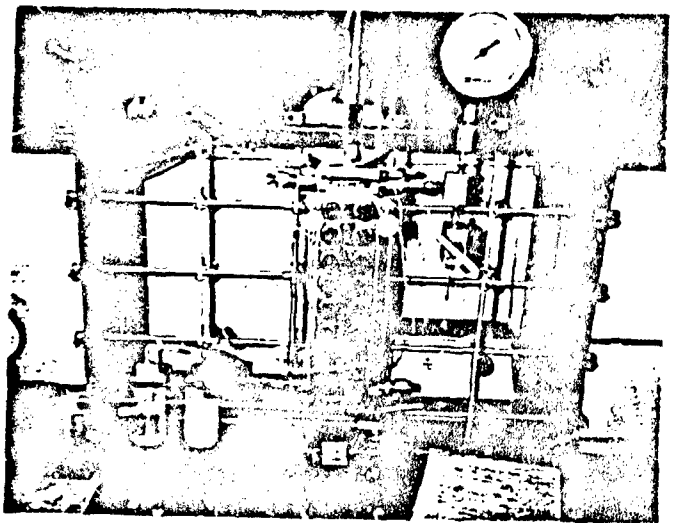

temperature, pressure, and concentration parameters, and the goals of the research were to determine these relationships. It is of value, however, to summarize some simple recrystallization theory insofar as the theory guided the experimental program in its early stages.

The equilibrium in assembly of dissolved molecules which can combine to form a critical nucleus beyond which size favorable fluctuations will cause the nuclei to grow has been described by Gibbs; he presented the conditions of critical nuclei formation based upon free energy considerations,[67], and Adamson[68] gives an excellent treatment of Gibbs' mathematical description. Since the formation of nuclei requires the formation of an interface between two phases, the free energy of the system will usually increase initially. Until an embryo (a particle smaller than a stable nucleus) reaches some critical diameter its growth demands that the interfacial energy increase. Once the particle is of sufficient size, i.e., of critical diameter, there are two competing modes of lowering the particle free energy: the nucleus can grow indefinitely, or it can shrink and disappear. It should also be considered that critical nuclei grow at the expense of subcritical embryos so that the final particle size is dependent upon the initial nuclei concentration. Adamson also presents a readable development of the rate equations describing nucleation first derived by Becker and Doring[68] Using the free energy considerations Becker and Doring derived an equation for the rate of formation of nuclei of this critical size, viz.,

$$\text{rate} = Ze^{-\Delta F_{max}/RT} \tag{1}$$

Z is the collision frequency (calculable from classical kinetic theory)

ΔF_{max} is the Gibbs expression which derives from nucleus surface energy considerations

The free energy relation is given by

$$\Delta F_{max} = B/[RT\ln s]^2 \tag{2}$$

B is a constant derivable from physical properties of the system.

s is the supersaturation ratio. (For purposes of illustration, in a vapor-liquid system s is the ratio of actual component pressure to the normal vapor pressure; in a system involving a solute dissolved in a solvent, s is the ratio of actual concentration to saturation concentration.)

From Eqs. 1 and 2 it is seen that the nucleation rate is very strongly influenced by the supersaturation ratio. As an example of the rapid increase in the rate, Adamson shows for the condensation of water vapor that the number of nuclei formed (per second per cc for water vapor at 0°C) is only 10^{-8} at a supersaturation ratio of 3.5 whereas it is 10^3 at a ratio of 4.5. The ratio

at which the nucleation rate changes from imperceptible (e.g., 10^{-8}) to very large (e.g., 10^{3}) is termed the critical* supersaturation ratio. The rate of nucleation at that point is termed catastrophic, and the phenomenon, catastrophic nucleation. That "some" level of supersaturation is necessary before embryo formation will occur is found in the observations of supercooling of polymer solutions, the requirement of the scratching of beakers to promote precipitation, seeding of clouds with silver iodide to promote rain (which is first formed as snow), etc.

Continuing with the quite general description of the total particle formation process, the size of the final particles achieved in any particular situation is governed by the rate of formation of critical nuclei and by the rate of growth of these nuclei. The kinetics of nuclei formation involves both free energy and rate of molecule transport at the interfacial boundary, the latter being especially difficult to describe in quantitative terms. The overall rate of growth of the nuclei once they have been formed during the catastrophic period can be given by the mass transfer relation

$$\text{flux of material to surface} = kA\,\Delta C \qquad (7)$$

- k is a mass transfer coefficient
- A is the surface area of the particle at any particular instant
- ΔC is the concentration driving force at any particular instant; it is given by $C-C_{eq}$ (or in words, the concentration of the component in the gas minus its equilibrium concentration.)

Thus, particle size and particle size distribution (PSD) is determined by the interaction between the nucleation rate and the growth rate of crystals, on one hand, and by the rate of creation of supersaturation, on the other hand. The interaction can be demonstrated by the schematic representation of competing events in Figure 11, in which supersaturation s is plotted against time. If supersaturation is created by the addition of an anti-solvent, the rate of addition will affect the rate of supersaturation creation, and it will be, of course, represented by the slope of the line in the graph.

There are three regions designated as the horizontal sections I, II, and III depicted in Figure 11. In region I the solution is undersaturated, i.e., the actual concentration is less than the thermodynamic equilibrium concentration, and no nucleation is taking place. In region II the solution is supersaturated but the supersaturation value is below the so-called critical supersaturation; no nucleation is observed, but any existing crystals in the mixture will grow. In region III both nucleation and growth are taking place.

*The word critical here is not related to the critical point of a gas or liquid.

FIGURE 11

SUPERSATURATION VS TIME IN PRECIPITATION BY CONTINUOUS ADDITION OF ANTI-SOLVENT

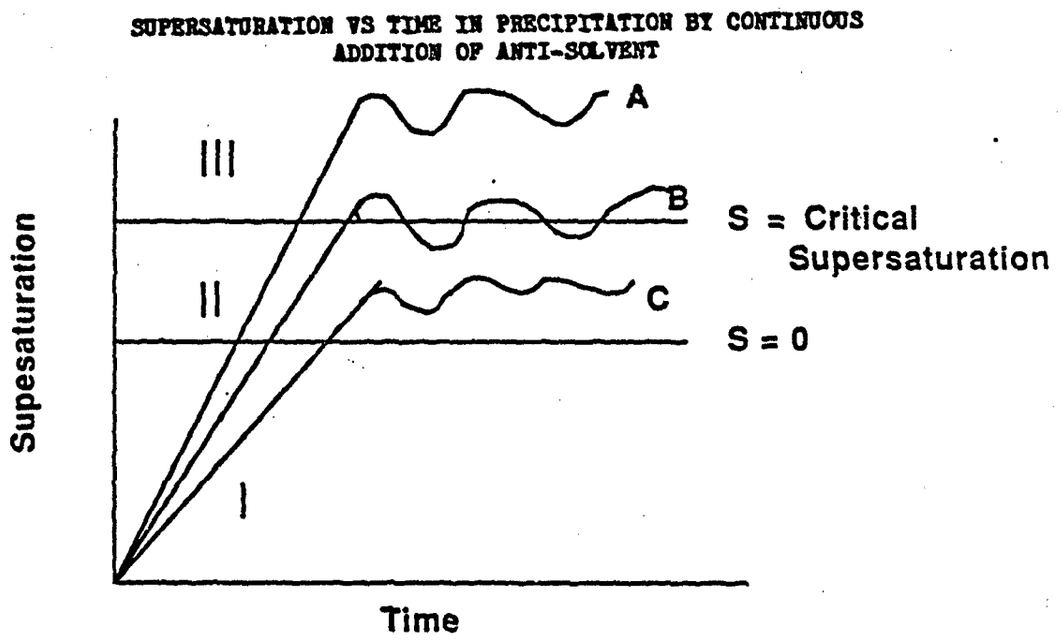

The size or the PSD of the precipitated crystals will depend on the nucleation rate and growth rate of the crystals (which are determined by the supersaturation, temperature, pressure, etc.) and the rate of supersaturation creation which is determined by the rate of anti-solvent addition, the original solute concentration in the solvent, and other factors. In other words, the particle size and PSD will depend upon the balance between the former processes which "consume" supersaturation and the latter, the generation of supersaturation.

Thus, in curve A the generation of supersaturation predominates over the consumption, and the system nucleates continuously (continuous polydisperse PSD), curve B represents cases with periodic nucleation events (discrete PSD), and in curve C nucleation takes place only in the beginning of the precipitation followed by growth (monodisperse or very narrow PSD). If in case C nucleation had been made to occur just above the critical supersaturation, a small number of nuclei would most probably form and consequently the final product would probably consist of rather large crystals of nearly uniform size which is the condition for the formation of large monodisperse crystals.

The rate of creation of supersaturation is related to the rate of expansion of the RDX-organic solution. The expansion of neat cyclohexanone, i.e., with no RDX in solution, and neat acetone was first determined in the sight glass. (The expansion was determined to guide subsequent "blind" tests carried out in the closed vessel assembly.) The volumetric expansion curves of cyclohexanone and acetone by carbon dioxide are shown in Figures 12 and 13. As the figures show, the volumetric expansion is quite large, and this phenomenon of absorption of carbon dioxide into these solvents and concomitant expansion is, of course, the basis for the supercritical fluid anti-solvent concept that was proposed and studied.

It is most facile and instructive to describe by means of photographs the expansion events that are observed in the sight glass during the introduction of supercritical fluid. The photographs will also give an indication of how the expansion curves in Figures 12 and 13 were obtained. Figure 14 is a photograph of the sight glass assembly, and the initial level of cyclohexanone is indicated by the arrow; a volume of 15 ml of cyclohexanone has been added to the cavity in the sight glass whose internal volume is 60 ml. Upon introduction of carbon dioxide the solution begins to expand and the per cent expansion at any pressure level is obtained from the observed level change and the volumetric calibration of the sight glass cavity. Figure 15 shows the expansion that has occurred at an arbitrary pressure level, 700 psig at 20°C, and the percent expansion can be calculated (and plotted as one point in Figure 12).

In order to determine recrystallization behavior and its relation to such factors as the extent of expansion at the onset of nucleation, etc., the sight glass assembly is again used. A cyclohexanone solution of RDX is contacted with carbon dioxide at increasing pressure in the same way as was the neat cyclohexanone, and the events that occur, e.g., nucleation as a function of extent of expansion are observed visually. It is again instructive to present

FIGURE 12 - VOLUMETRIC EXPANSION OF
CYCLOHEXANONE BY CARBON DIOXIDE

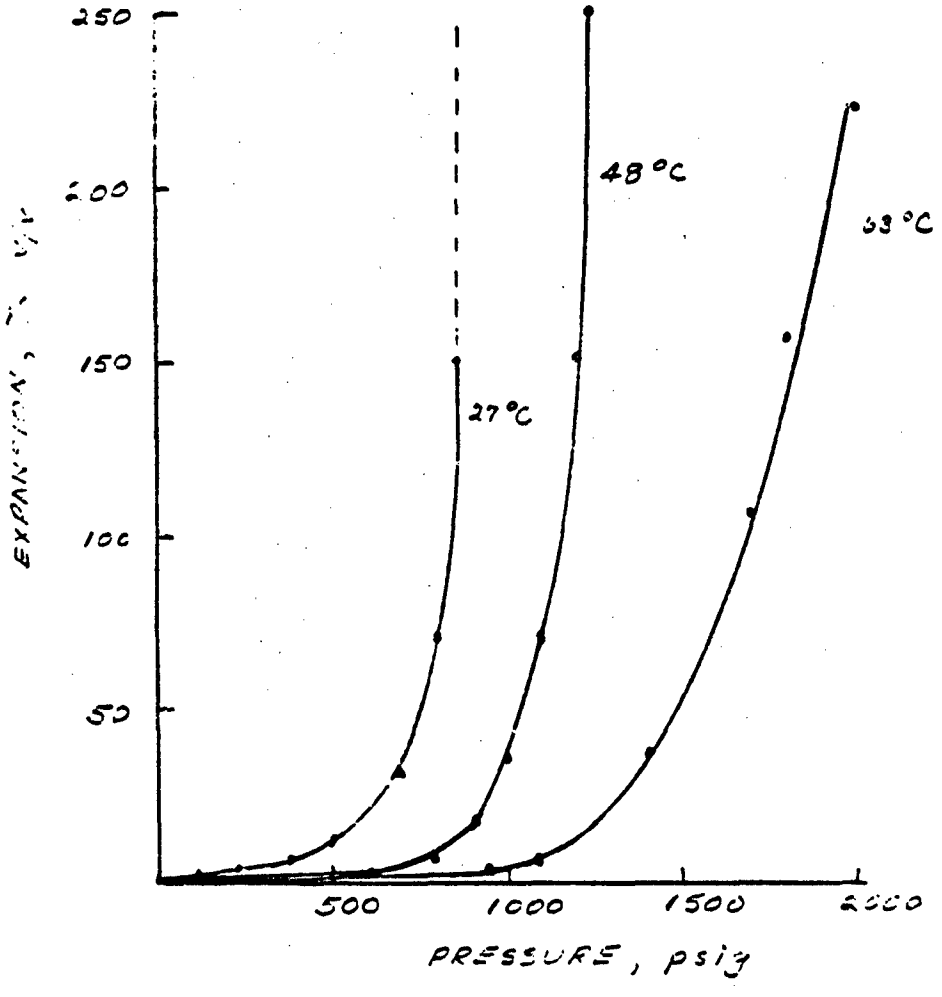

FIGURE 13 - VOLUMETRIC EXPANSION OF ACETONE BY CARBON DIOXIDE

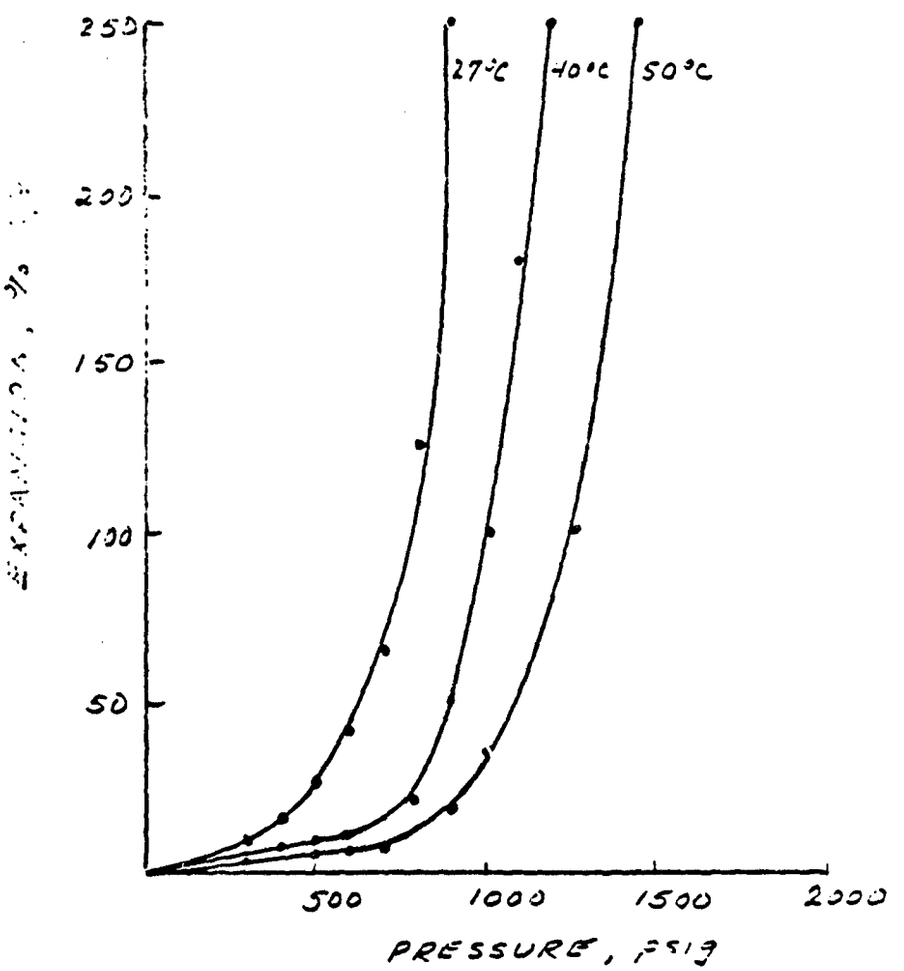

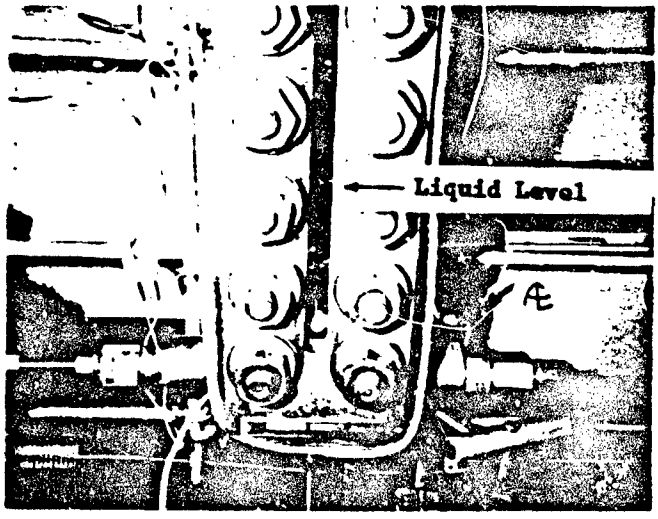

FIGURE 14 - SIGHT GLASS SHOWING INITIAL LEVEL OF CYCLOHEXANONE

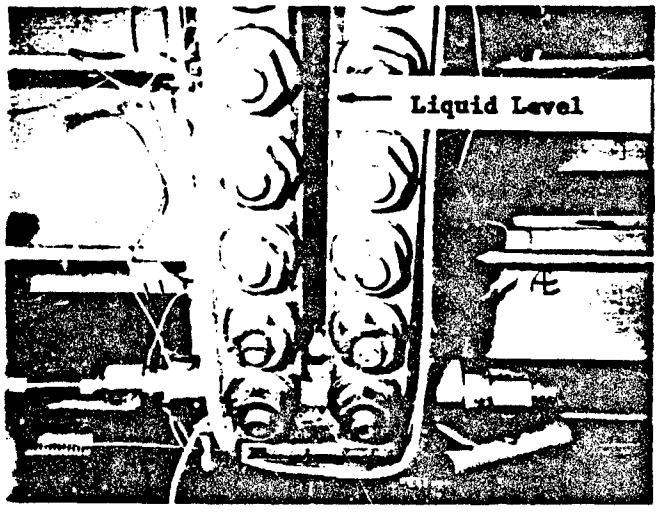

FIGURE 15 - SIGHT GLASS SHOWING LEVEL OF CYCLOHEXANONE AND CARBON DIOXIDE AT 700 PSIG

the events that are observed by means of photographs. Figure 16 is a photograph of the sight glass that has been charged with 15 ml of 10% RDX-cyclohexanone solution; the initial level of the solution is indicated and the axial mixing action was not energized for this test. As carbon dioxide is admitted, the solution expands as the gas dissolves in the organic liquid. At some sufficiently high extent of expansion minute crystals are seen to form. Figure 17 depicts this condition, and the level of the solution is indicated. The solution has become hazy because of the presence of small particles of RDX, and this condition is termed "onset of nucleation". For strict accuracy, here, the turbidity of Figure 17 is "slightly" beyond the true onset so that a more visible condition could be photographed. At the true onset of catastrophic nucleation that is governed by the thermodynamic and kinetic factors discussed earlier, the actual nuclei themselves are not visible since in theory they comprise assemblies of "a few" thousand molecules. The appearance of the visible haze nonetheless was a convenient measure in the laboratory of the effects of changes in parameters.

Digressing for the time being from further discussion of the recrystallization experiment whose start was shown in Figures 16 and 17, it is of value to discuss the "onset of nucleation" condition further here in order to present how it is related to the extent of volumetric expansion and how still other factors such as the rate of introduction of gas can influence both this onset condition and the size and shape of the crystals ultimately formed. In the particular experiment whose photographs are shown in Figures 16 and 17, the gas pressure level of 700 was reached within a few seconds because of the particular rate of introduction of the gas. If on the other hand, the gas is introduced at a much lower rate, say, over a period of the order of a few minutes, the onset of nucleation is seen to occur at about 100 psi or more lower; additionally, during the slow introduction it is seen that the degree of turbidity is not so great at onset which is an indication that fewer particles are being formed at that particular time. In fact, in the slow addition case the number of particles that are seen to form to a size to be visible are so few as to almost defy detection; they are identified to be present in the liquid by the expedient of moving the backlighting to various levels and angles and visually determining the light reflected from the crystals.

In brief summary here, then, even the "relatively simple" observation of the onset of nucleation is in some way related to a pressure-time function. The number of crystals observed to form is also related to pressure-time, and assuredly so is the size and shape of the crystals. The phenomenon is quite complex, but size-shape phenomena can be related experimentally to a number of parameters which can be selected and controlled, and results of photomicrographic analysis are presented subsequently.

Returning, now, to the discussion of the recrystallization experiment shown in Figures 16 and 17, to complete the test to precipitate all (or almost all) the RDX that was in solution the pressure is raised still further causing the solution to expand still further, causing in turn a still further decrease in the solvent power of the cyclohexanone phase for RDX which, of course, results in both crystal growth and additional nucleation. The results of reaching a pressure level of 850 psig is shown in Figure 18. The

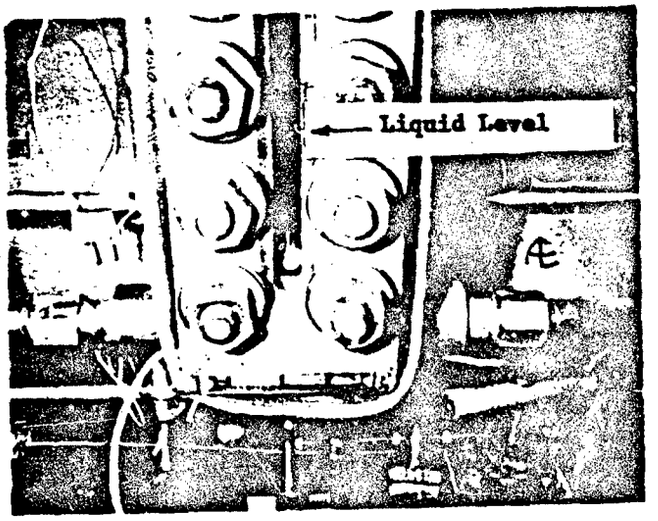

FIGURE 16 - SIGHT GLASS AND INITIAL LEVEL OF RDX-CYCLOHEXANONE SOLUTION

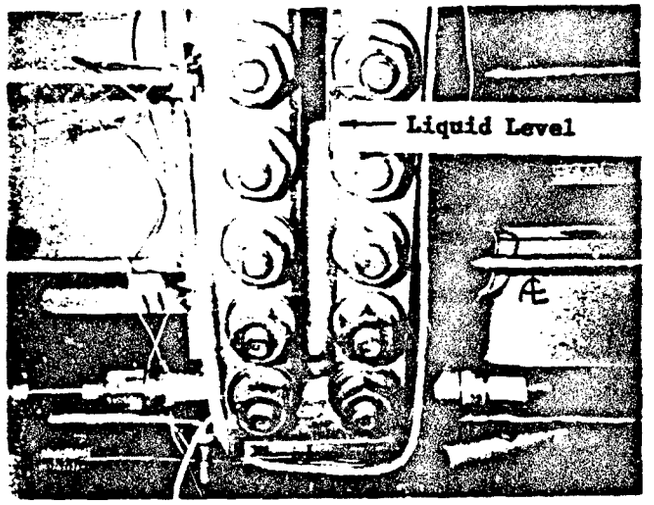

FIGURE 17 - SIGHT GLASS SHOWING ONSET OF NUCLEATION AT 700 PSIG CARBON DIOXIDE

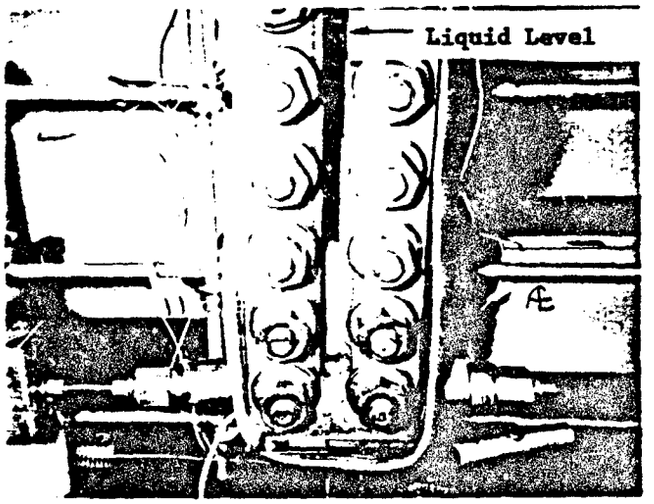

FIGURE 18 - SIGHT GLASS SHOWING FULL EXPANSION AND SETTLING OF RDX CRYSTALS

cyclohexanone has expanded almost two-fold and most of the RDX crystals have settled and have collected at the bottom of the sight glass cavity. To obtain a sample for micrographic analysis the cyclohexanone-carbon dioxide phase is drained through the port below the cotton plug, and the crystals collect on the cotton. The crystals are "washed" once (or more times) by the expedient of introducing more gas to its liquefaction point, and the adhering cyclohexanone is dissolved. Draining the carbon dioxide (which now contains the previously adhering cyclohexanone) results in virtually dry RDX crystals which are removed from the sight glass by means of a long handled spatula.

The sample of recrystallized RDX is prepared for microscopy evaluation by placing a very small amount of the RDX on a drop of toluene that had been placed on a glass slide with a fine tip dropper, dispersing the powder and drop of toluene, and spreading the dispersion on the glass slide to ensure that the particles are distributed and a cover slide placed on the dispersion. The slide is dried (to evaporate the toluene), a drop of a dispersion oil is distributed over the particles, and a cover slide placed on this dispersion. The particles are examined with transmitted light. The refractive index of the two dispersion oils used was 1.500 and 1.600, respectively; the refractive index of RDX crystals ~1.598, 1.602, and 1.585, respectively, for the three crystal faces. The crystals will be somewhat difficult to distinguish in some of the photographs, therefore, but any intragranular inclusions will appear as dark (or opaque) spots. Photomicrographs were taken at primarily two magnifications, 150X and 300X, which convert to scale markers of 15 mm/100 microns and 30 mm/100 microns, respectively.

Figures 19a and 19b are photomicrographs of the as supplied RDX produced by Holsten Army Ammunition Plant. (The written notes on the photographs are the microscopist's designation for test number, file number, magnification, etc., and are retained for ease of comparison of the magnification and scale marker.) The average particle size is seen to range from about 10 microns to 400 microns, and almost all the crystals contain intragranular cavities. These cavities are seen to be quite large, in some instances, of the order of 20-50 microns or more. These cavities are voids that result when the liquid that has been trapped in the crystal during the crystal growth process evaporates/diffuses from the crystal; as stated in the Summary, it was the formation of RDX crystals without voids that was the goal of this program. As related in Section I the main objective of the program was to investigate the gas anti-solvent recrystallization process for its potential to form 100 - 150 micron cavity-free RDX. During a site visit early in the program by Drs. Warren Hillstrom and Robert Frye and a demonstration of the capabilities of the process, especially as to the ease of formation of very small particles, less than, say, 10 - 20 microns, the program was modified so as to include also the investigation of parameters which would form RDX of controlled small size. The discussion of results that follows includes both aspects. As is shown, the process can be tailored to produce both small and large particles of intragranular cavity-free RDX.

Depending upon the factors and parameters mentioned earlier, viz., pressure, temperature, concentration of RDX, rate of introduction of gas, etc., a variety of shapes and sizes of crystals could be formed by the supercritical fluid anti-solvent process. As was discussed previously in a

FIGURE 19a -

RDX CRYSTALS PRODUCED AT HOLSTEN AAP. OPAQUE SPOTS ARE INTRAGRANULAR CAVITIES

5437-5 RDX Control $n_D = 1.602$ 60X

FIGURE 19b -

LARGER MAGNIFICATION OF RDX CRYSTALS MADE TO ACCENT THE SIZE OF INTRAGRANULAR CAVITIES

5433-1 RDX Control 150X

general way, a rapid increase in the supersaturation ratio will lead to a high nucleation rate, a large depletion of solute concentration, and concomitant small particles. A rapid introduction of gas into the vessel causes rapid expansion of the solution, and the expansion, of course, lowers the dissolving power of the cyclohexanone, which is equivalent to an increase in supersaturation. As was shown visually in Figures 16, 17, and 18, if carbon dioxide is injected to some pressure beyond that "threshold" pressure (THP) at which particles first can be seen to appear, the nucleation is massive and occurs almost instantaneously, depleting the solution in RDX. Accordingly, in this case, the final particle size is small due to the lack of material available for subsequent growth, and the PSD is quite narrow. Figure 20 shows the general trend for recrystallization with rapid injection. Importantly, very few of the RDX crystals show evidence of the opaque spots that are indicative of the intragranular cavities.

Threshold pressures (which are near where the expansion curve becomes exponential) at various RDX concentrations were determined by observation in the sight glass. It was found that when RDX solution concentration is decreased, the pressure required for onset of nucleation increases, or stating this result differently, the lower the concentration the higher the extent of expansion required to cause RDX to nucleate. Figure 21 is a graph of the extent of expansion required to cause onset of nucleation for RDX concentration in cyclohexanone. The trend is quite easy to explain. At high RDX concentration very little anti-solvent (i.e., very little expansion) is required to begin to precipitate the RDX because a supersaturation condition is reached quickly as carbon dioxide is injected. At the very low concentration end a large amount of expansion is necessary to reach a supersaturation condition. These results are analogous to the events during the precipitation that, for example, occurs by cooling of RDX solutions of two respective concentrations, viz., a high concentration one and a low concentration one. If, for example, a solution of RDX in cyclohexanone saturated at, say 80°C, is cooled, a drop in temperature of only a few degrees will result in the formation of crystals. If a low concentration solution, say, 1%, is cooled from an initial temperature of 80°C, no precipitation will occur until some very cold temperature probably well below room temperature is reached.

With slow injection of the gas, of the order of 3 to 5 min, nucleation begins to occur again at the "threshold" pressure (THP); onset of nucleation and THP are used interchangeably in subsequent discussion. The particles that are formed depend upon the procedure that is followed after the onset of nucleation at the threshold pressure. If gas injection is terminated at the THP (and after onset has occurred) and the system is allowed to remain for some hold time, the nuclei that are formed will grow. Because fewer nuclei are formed at this condition than in the case of rapid injection far beyond the threshold pressure the crystals can grow much larger. Figures 22a and 22b show that very large crystals can be produced. Figure 22a shows RDX recrystallized from cyclohexanone and 22b from acetone. Some very small cavities are seen in the crystals formed from acetone solution, but as seen from Figures 20 and 22a and as will be seen subsequently, very few intragranular cavities are present in RDX recrystallized from cyclohexanone. In the slow injection situation when gas injection is continued beyond THP,

FIGURE 20 - TYPICAL RDX CRYSTALS PRODUCED WITH RAPID INJECTION OF CARBON DIOXIDE INTO RDX - CYCLOHEXANONE SOLUTION

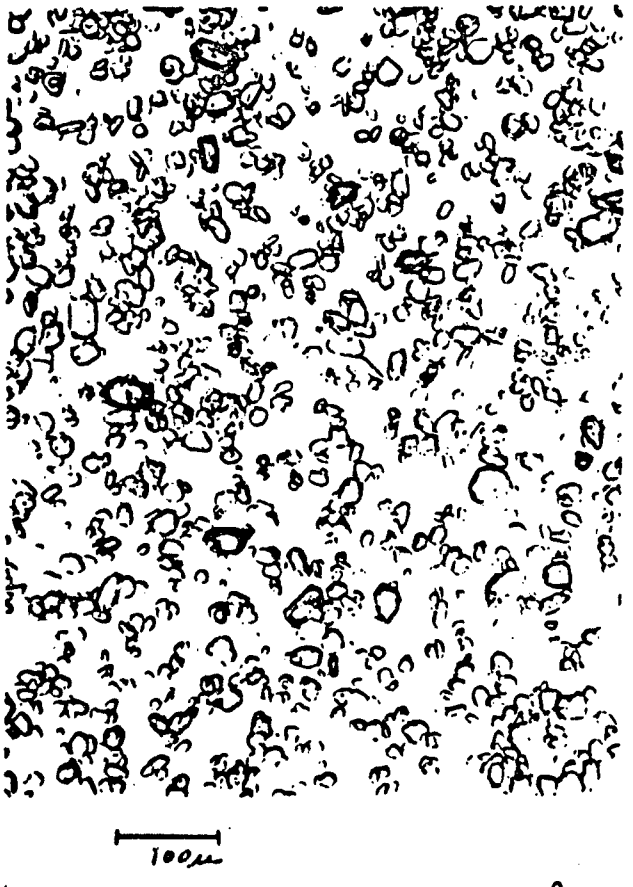

FIGURE 21 - VOLUMETRIC EXPANSION REQUIRED OF RDX-CYCLOHEXANONE SOLUTIONS TO CAUSE ONSET OF NUCLEATION

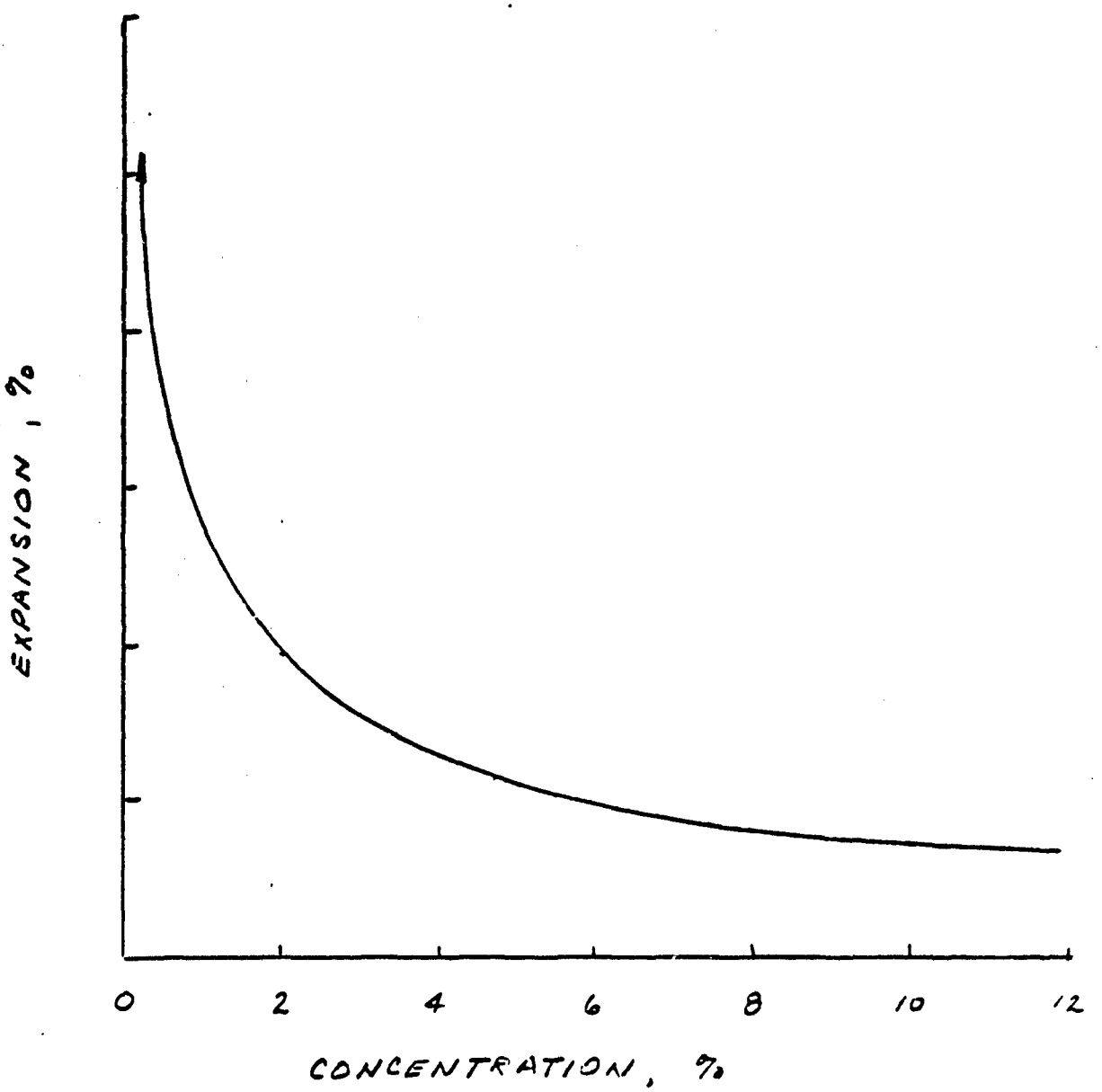

FIGURE 22a -

TYPICAL CRYSTALS PRODUCED FROM RDX-CYCLOHEXANONE SOLUTION WITH SLOW INJECTION AND LONG HOLD AT ONSET OF NUCLEATION

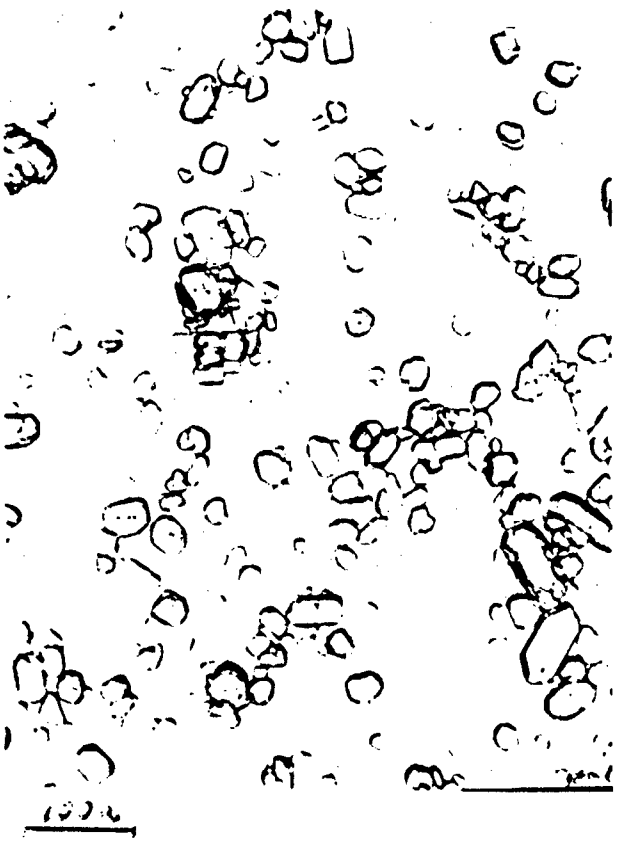

FIGURE 22b -

TYPICAL CRYSTALS PRODUCED FROM RDX-ACETONE SOLUTION WITH SLOW INJECTION AND LONG HOLD AT ONSET OF NUCLEATION

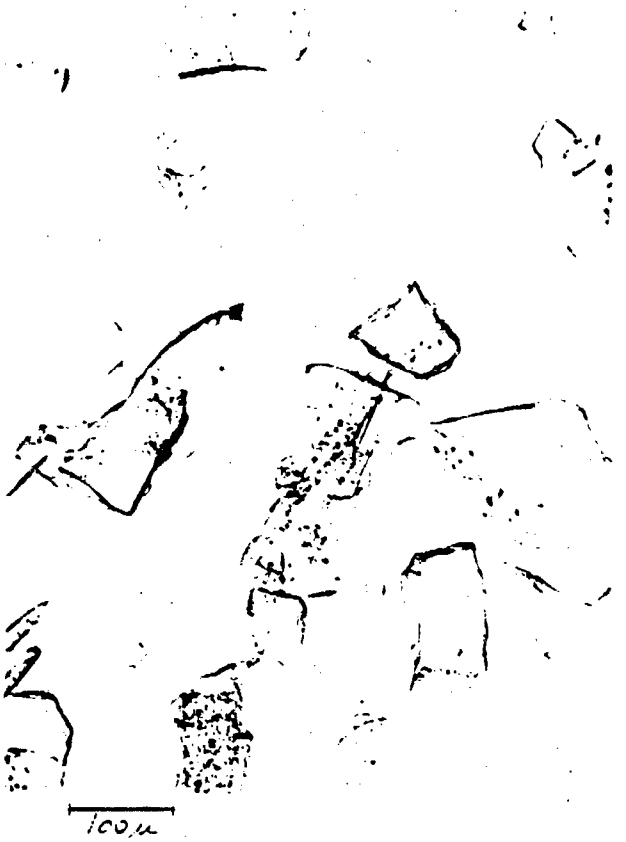

FIGURE 23 - TYPICAL CRYSTALS PRODUCED FROM RDX-ACETONE SOLUTION WITH SLOW INJECTION CONTINUING PAST ONSET OF NUCLEATION (WIDE PARTICLE SIZE DISTRIBUTION)

the simultaneous occurrence of "new" nucleation and continuing growth produces a very wide distribution of particle sizes. Figure 23 shows RDX crystals formed during slow carbon dioxide injection beyond THP; they range from tens to hundreds of microns in size.

The generalizations made above are sufficient for describing the resultant particle size and PSD for almost all subsequent tests. In brief summary, with rapid injection beyond threshold pressure it is understood that particles will be fairly small and PSD fairly uniform regardless of hold time. In discussing the various sets of results, the designation rapid (30-60 sec) or slow (3-5 min) gas introduction will be referred to. In some of the slow injection tests in order to ensure that the particles grow as much as possible and also to provide some semblance of "time control", a hold time of ~20 min was used; this is designated "long" hold time (unless otherwise indicated).

One of the most significant variables to consider is the choice of solvent, since the final particle size, PSD, and yield (recovery of RDX crystals from solution) are influenced by the solubility of RDX in the organic solvent. Table III shows the temperature-RDX concentration pattern for two solvents that are used in the manufacturing process at Holsten AAP. (Many other common solvents such as the paraffins and aromatics exhibit virtually no dissolving power for RDX.)

TABLE III

Solubility of RDX in Organic Solvents

	T°C	Solubility (g/100g)
Acetone	20	7.3
	40	11.5
	60	18.0
Cyclohexanone	25	12.7
	97	25

Regardless of the operating conditions, there is a startling difference between recrystallization of RDX from acetone and from cyclohexanone. With only a few exceptions use of cyclohexanone as the solvent produces smaller regular-shaped particles, whereas with acetone the particles were quite irregular and sometimes hundreds of microns in size at the same external conditions of temperature, pressure, rate of injection of gas, etc. The reasons for these differences are not known at present, and these differences are considered somewhat surprising. Table IV, page 73 from an Aberdeen PG report (AMCP706-177) is a listing of solvents, RDX solubility, and the crystalline form of RDX that is recrystallized from the solvents by the "normal" procedures described earlier. The table shows that thick hexagonal crystals are formed from acetone solution, and thick hexagonal is the form of

TABLE IV

Solubility and Crystal Form of RDX

Cyclonite (RDX)

Solubility of Cyclonite, Holston Lot E-2-5 in Various Solvents:

Solvent	Boiling Point, °C	Grade or Source*	Solubility gm/100 gm Solvent 28°C	Heated	Crystalline Form
Acetone	56	CP	8.2	16.5 at 60°C	hexagonal-thick
Cyclohexanone	155.6	CP	13.0	24.0 at 93°C	cubic (massive form)
Nitromethane	100.8		1.5	12.4 at 97°C	plates
Acetonitrile	81.6	Miacet Chem. Co.	11.3	33.4 at 93°C	plates
1-Nitropropane	126.5	EK Pract	1.4	10.6 at 93°C	short needles
2-Nitropropane	120	EK Pract	2.3	11.6 at 93°C	short needles
2,4-Pentanedione	140.5	Carbide & Carbon	2.9	18.3 at 93°C	flat prisms
Methylisobutylketone	115.8		2.4	9.6 at 93°C	long prisms
n-Propylacetate	101.6	EK Red Label	1.5	6.0 at 93°C	long prisms, some cubic
n-Butylformate	105.6	EK Red Label	1.4	4.6 at 93°C	long prisms
Ethyl acetate	77.1	Baker's CP	2.0	6.1 at boil.	hexagonal plates
n-Propylpropionate	121	EK Red Label	0.8	1.6 at 93°C	short prisms, some cubic
Butylacetate	126.5	EK Technical	1.1	4.0 at 93°C	long prisms
Methylethylketone	79.6		5.6	13.9 at boil.	coarse plates
Nitroethane	114.2	EK Red Label	3.6	19.5 at 93°C	plates
Isopropylacetate	88-90	CP	1.1	3.2 at boil.	long prisms
Mesityloxide	128	EK Red Label	4.8	14.5 at 93°C	plates
n-Amylacetate	146	CP	1.0	2.1 at 93°C	prisms
Dimethylcarbonate	88-91	EK Red Label	1.4	6.6 at boil.	plates
Diethylcarbonate	125-126.5	EK Red Label	0.7	3.2 at 93°C	prisms
Isoamylacetate	132	CP	1.2	3.6 at 93°C	prisms
Ethylpropionate	98-100	EK Red Label	3.0	10.7 at 93°C	fairly thick hex plates
Methyl-n-butyrate	101.5-103.5	EK Red Label	1.2	4.9 at 93°C	needles
Cyclopentanone	130.6	EK Red Label	11.5	39.0 at 93.5°C	hexagonal plates
Acrylonitrile	77.3	Cyanamid Co.	4.0	16.4 at boil.	flat plates
Methylcellosolveacetate	144.5	Carbide & Carbon	1.6	8.8 at 93°C	massive hexagons and prisms

* EK, Eastman Kodak; Pract, practical.

crystal seen in Figure 22b which is recrystallized from acetone by carbon dioxide injection. The table shows that cubic crystals are formed from cyclohexanone solution, and interestingly, the crystals formed by carbon dioxide injection into cyclohexanone solution are also reasonably cubic as is seen in Figures 20 and 22a. As further interesting information Table IV shows that "normal" recrystallization of RDX from two closely related solvents, viz., cyclohexanone and cyclopentanone, produces quite different crystals.

Concerning the size of crystal one might expect that because more RDX can dissolve in cyclohexanone, at room temperature, for example, larger RDX particles would result since there would be relatively more material available for growth after some initial nucleation. Apparently, with RDX-cyclohexanone solutions more nuclei form at the threshold pressure relative to the events using acetone under similar conditions. Figures 24a and 24b and Figures 25a and 25b are photomicrographs of RDX recrystallized from cyclohexanone with rapid injection of CO_2 over a wide range of temperature and pressure. As was shown earlier in Figure 20, very small particles with extremely uniform PSD can be produced (and reproduced). The initial RDX-cyclohexanone concentration for this series of tests is at the saturation for the corresponding temperatures. These photomicrographs show that at any temperature increasing maximum operating pressure doesn't change final particle size or PSD as long as THP is surpassed.

On the other end of the particle size spectrum, recrystallization of RDX from acetone with slow injection of carbon dioxide produces very large crystals, and Figures 26a and 26b show examples of some of the largest RDX crystals produced on the program. Although at first glance the operating conditions given appear very different, both tests were conducted with solutions near-saturation (at each corresponding temperature) and the maximum operating pressure is the THP with a long hold time. Crystals of RDX formed from cyclohexanone have (except for a few particles, almost no opaque spots in them, indicating that few intragranular cavities are formed by the gas anti-solvent recrystallization process. Similarly only very few of the RDX crystals formed from acetone solution exhibit intragranular cavities and, in general, they are very small (although in a few crystals they are quite numerous).

As was explained earlier continuing a slow gas introduction beyond THP (for each RDX concentration and temperature) gives a product with a broad range of particle sizes. Figures 27a, 27b, and 27c depict results of different parameter combinations, again from acetone. Particles range from many of five micron size (barely visible in the figures) to 100-150 microns.

In some of the tests that were carried out some unusual morphology or quite peculiarly-shaped crystals were formed. Some of the shapes could be explained and some were not, but for completeness and interest value, the next few figures present some quite diverse particle shapes.

On some occasions large, thin platelets were formed, and initially there seemed to be no correlable factors to explain the platelets. Figures 28a and 28b are photomicrographs of platelets recrystallized from cyclohexanone. Table IV and all the other figures which reproduced cyclohexanone-

FIGURE 24a - RDX CRYSTALS - RAPID INJECTION INTO RDX-CYCLOHEXANONE (11.3% RDX, 25°C, 1000 psi)

FIGURE 24b - RDX CRYSTALS - RAPID INJECTION INTO RDX-CYCLOHEXANONE (15.0% RDX, 50°c, 1500 psi)

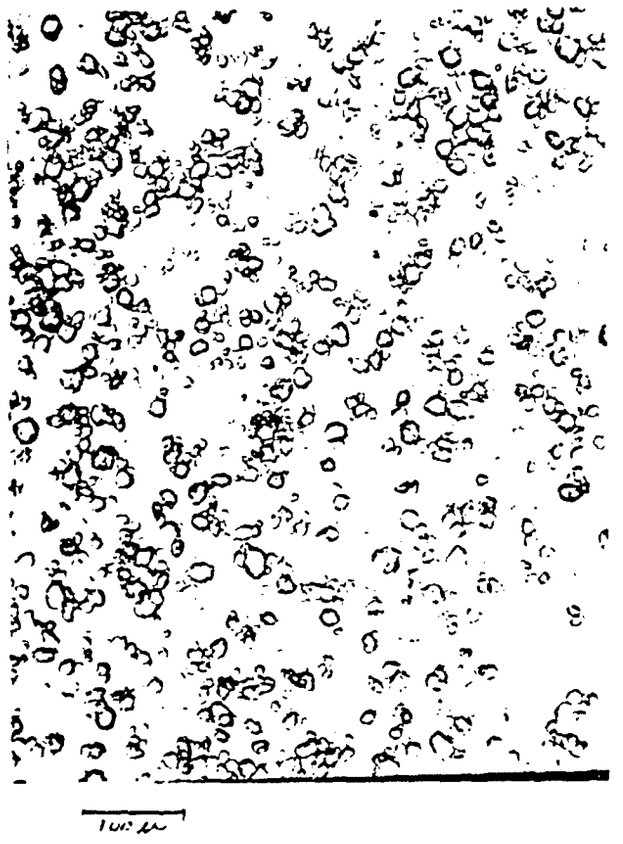

FIGURE 25a - RDX CRYSTALS - RAPID INJECTION INTO RDX-CYCLOHEXANONE (13.5% RDX, 50°c, 2300 psi)

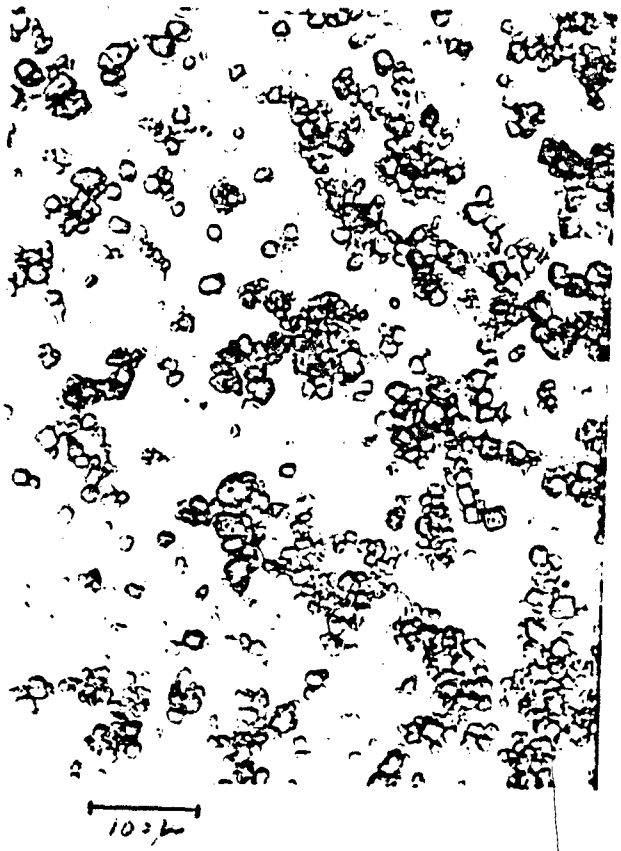

FIGURE 25b - RDX CRYSTALS - RAPID INJECTION INTO RDX-CYCLOHEXANONE (13.2% RDX, 60°c, 2300 psi)

FIGURE 26a - RDX CRYSTALS - SLOW INJECTION INTO RDX-ACETONE (12% RDX, 35°c, 1000 psi)

FIGURE 26b - RDX CRYSTALS - SLOW INJECTION INTO RDX-ACETONE (7% RDX, 20°c, 500 psi)

55

5374-C nD = 1.515 150X

FIGURE 27a – RDX CRYSTALS FORMED FROM ACETONE SOLUTION – SLOW INJECTION BEYOND THRESHOLD PRESSURE
(9.5% RDX, 22°c, 900 psi)

FIGURE 27b – RDX CRYSTALS FORMED FROM ACETONE SOLUTION – SLOW INJECTION, SHORT HOLD AT THRESHOLD PRESSURE, THEN CONTINUED INJECTION
(15.6% RDX, 40°c, 1200 psi)

FIGURE 27c – RDX CRYSTALS FORMED FROM ACETONE SOLUTION, LONG HOLD TIME AT THRESHOLD PRESSURE, THEN CONTINUE INJECTION (6.8% RDX, 22°c, 760 ps

17 C D

N 19 150x

GURE 28a - THIN PLATELETS OF RDX OCCASIONALLY FORMED FROM RDX-CYCLOHEXANONE

FIGURE 28b - THIN PLATELETS OF RDX OCCASIONAL FORMED FROM RDX-CYCLOHEXANONE

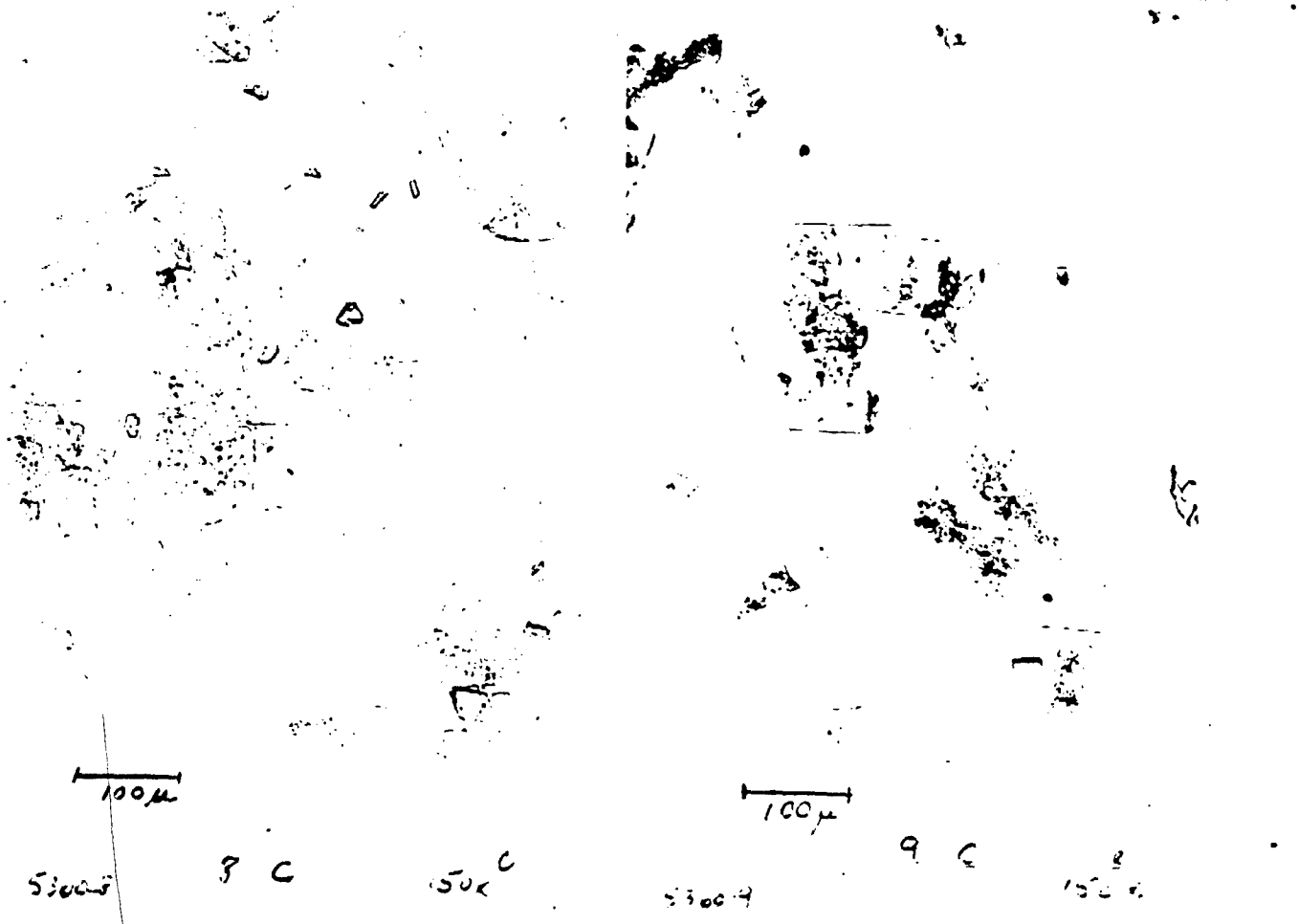

recrystallized RDX showed that regular (cubic) crystals are produced from cyclohexanone solution, and thus the platelets are a priori anomalous. Crystallization tests that were carried out in the sight glass provided information on the (occasional) appearance of the platelets, and it is most facile to refer to a series of diagrams in Figure 29 in order to explain the formation of platelets. Figure 29a points out the initial level of RDX-cyclohexanone, and Figure 29b the level after introduction of carbon dioxide to a point short of onset, i.e., no haziness has appeared in the expanded solution. If the gas has been introduced very rapidly, say of the order of a few seconds, the "bubbles" of carbon dioxide mixing with the cyclohexanone are large; the small surface area per unit weight of the gas impedes mass transfer to the solution, and thus, the cyclohexanone and gas are not at equilibrium at the top of the solution (nor in the bulk of solution). If the carbon dioxide flow is stopped and the system allowed to remain quiescent at the conditions of Figure 29b another "zone" appears at the surface of the expanded solution. This zone is distinguished by a "refractive index interface" and is a result of additional absorption of carbon dioxide into the not-completely-expanded cyclohexanone-RDX solution. The higher concentration of carbon dioxide in this layer is responsible for the difference in refractive index which the eye can distinguish; Figure 29c shows this zone. As the absorption and diffusion continues, the zone increases in thickness as depicted in Figure 29d. At "some" condition of absorption, of gas, platelets of RDX were seen to form at the interface; when the platelets grew to a sufficient size, they disengaged from the diffusion layer and fell to the bottom of the sight glass cavity; Figure 29e depicts this situation, viz., the growth of the platelets, their disengagement from the interface, and the settling to the bottom of the sight glass.

A very peculiar collection of platelets is shown in Figure 30. The interior of the platelets are essentially cavity-free, but they consist of a perimeter zone of tiny cavities. (Interestingly, thin platelets in Figure 28 also have tiny intragranular cavities.) Replication of this peculiar crystal was not explored, but in the particular test that produced the platelets shown in Figure 30, the pressure was increased then decreased several times, i.e., a pressure near the threshold pressure was reached and maintained for several minutes, then the pressure was decreased, and the procedure repeated several times. It is conjectured that platelets formed during the first pressure increase and that during the second (or third) cycle more RDX was formed heterogeneously on the first crystals. Why the "new" RDX is so cavity-laden is not explainable; nevertheless, the crystals are quite interesting in appearance. Other peculiarly-shaped crystals are shown in Figures 31a and 31b. Figure 31a is a photomicrograph of RDX needles recrystallized from cyclohexanone, and Figure 31b shows some needles and other crystals recrystallized from acetone; note the large (500 micron X 100 micron) thin platelet in the upper right hand corner. It is barely visible in the 1.500 immersion fluid, but it is seen to be absent of cavities.

In summary of all the results, the use of supercritical fluid anti-solvents has been shown to be an effective concept to recrystallize RDX from solution. The RDX that was used in the tests contained large cavities (cf. Figures 19a and 19b but particles containing virtually no intragranular cavities can be formed by the process, and the process can be tailored to

FIGURE 29

Schematic Diagram of Sight Glass Tests

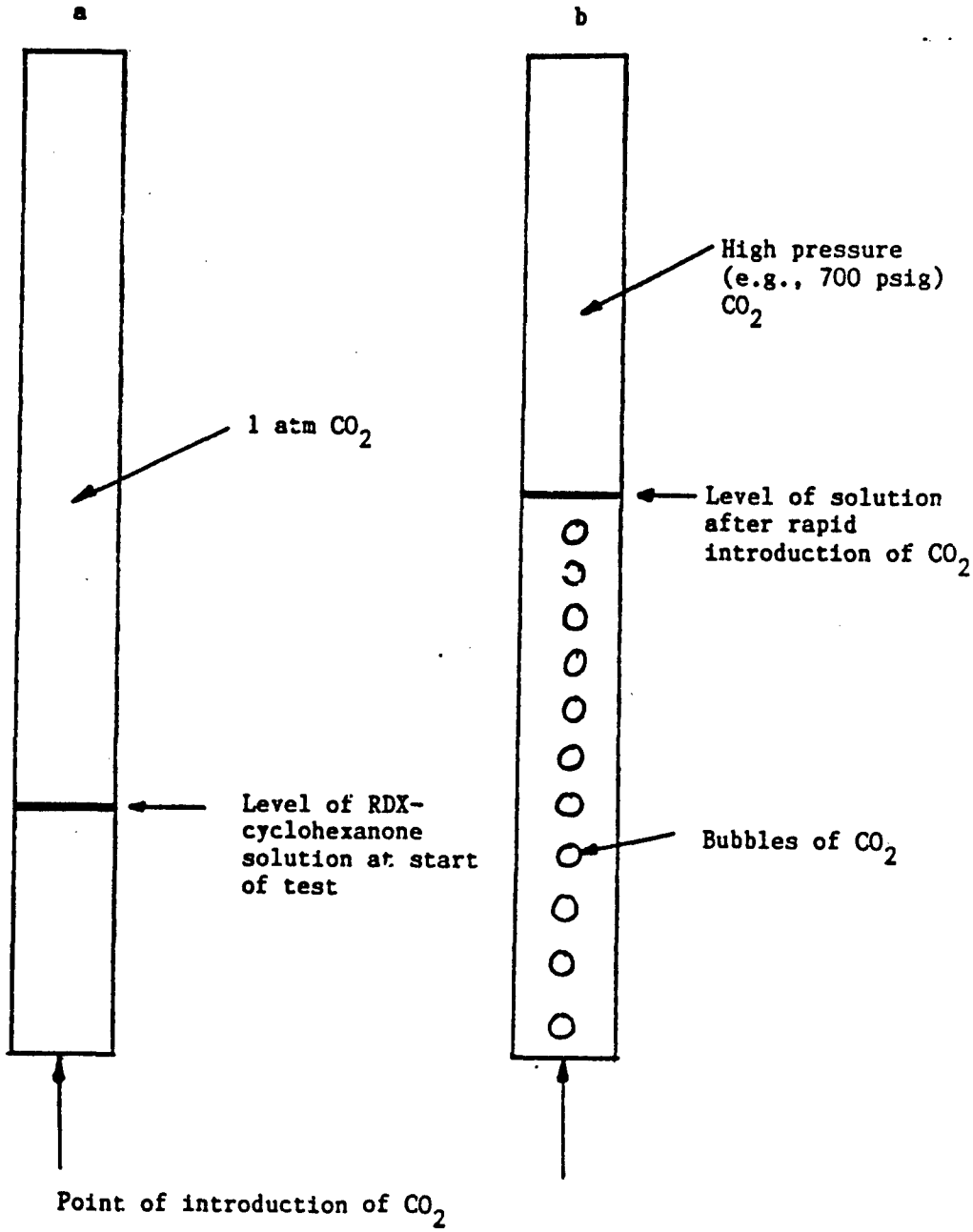

FIGURE 29

Schematic Diagram of Sight Glass Tests

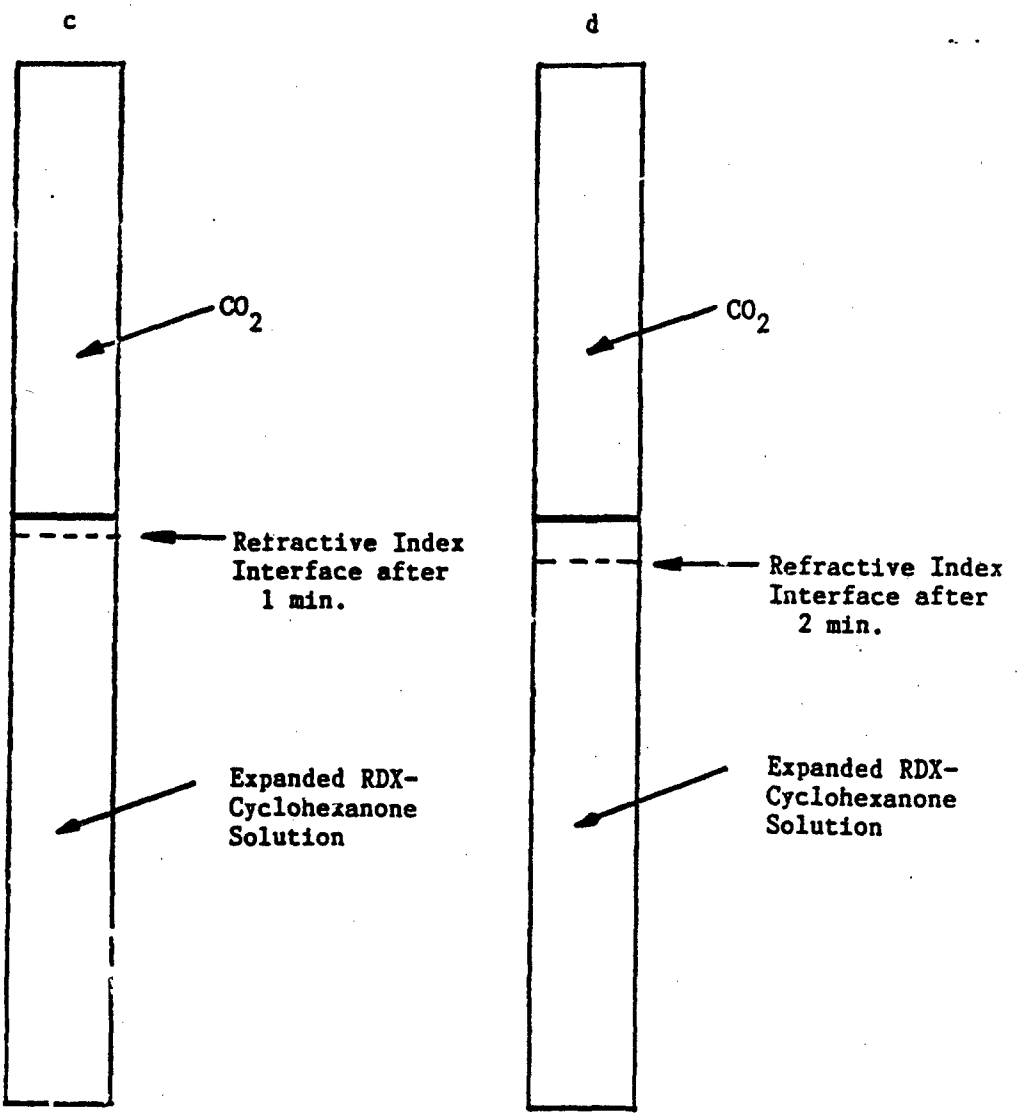

FIGURE 29

Schematic Diagram of Formation of Platelets of EDX

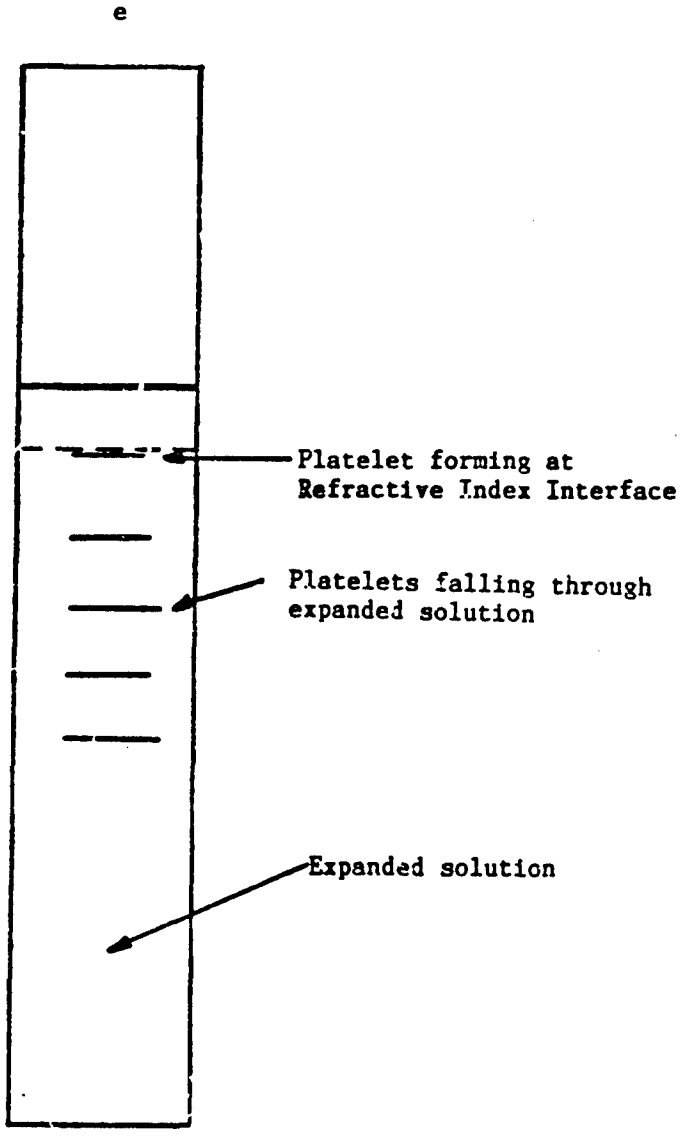

FIGURE 30 - PLATELETS OF RDX FORMED FROM RDX-CYCLOHEXANONE SOLUTION

47c 150x

FIGURE 31a

NEEDLES OF RDX FORMED FROM RDX-CYCLOHEXANONE SOLUTION - SLOW INJECTION TO THRESHOLD PRESSURE AND HOLD (VERY HIGH TEMPERATURE SOLUTION, 80°C, 20% RDX, 2500 psi)

FIGURE 31b

UNUSUAL RDX CRYSTALS FORMED FROM ACETONE SOLUTION (6% RDX, 20°C, 800 psi)

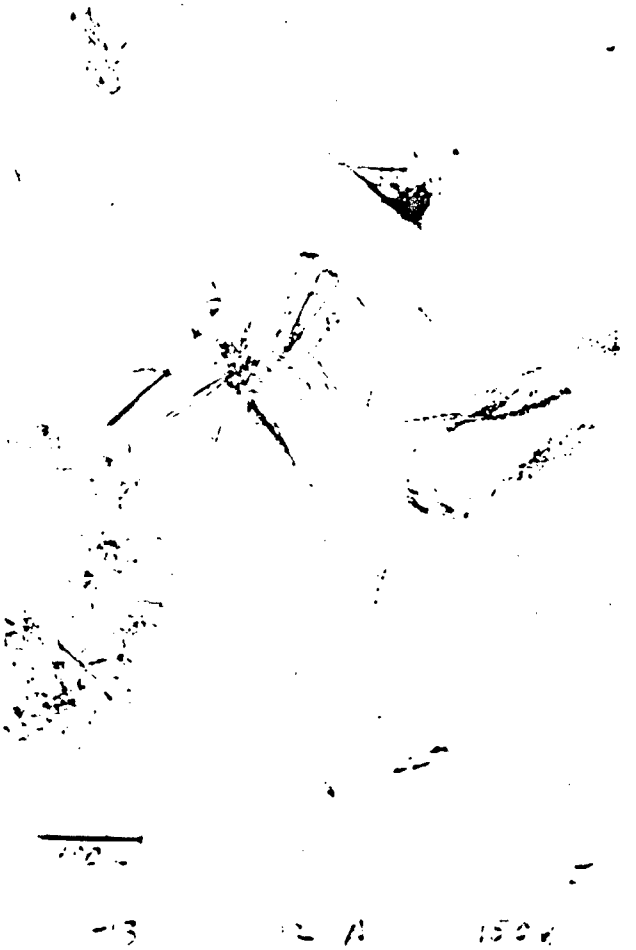

produce RDX of controlled size and particle size distribution. Some quite unusual crystals formed and shown in Figures 28-31 were presented primarily for their interest value and completeness of results obtained on the program.

There are other variations of the gas anti-solvent process that are described here. Figure 21 showed that the onset of nucleation is strongly influenced by the concentration level of RDX in solution. Extrapolating from this figure then, if two materials, say, RDX and a polymer, are dissolved in a solvent, it should be possible to co-precipitate the materials, or to coat one with the other. For the coating variation, RDX would be dissolved to a "high" concentration level and the polymer to a "low" concentration level. Gas can be injected to a sufficient expansion level to recrystallize the RDX, then gas injection continued to an expansion level sufficient to "recrystallize" the polymer. The respective initial concentration levels are not now known, but some preliminary feasibility tests could establish the limits. It is speculated that the presence of the recrystallized RDX in suspension will serve as heterogenous nucleating sites for the polymer resulting in a quite uniform coating.

The economics of the gas anti-solvent recrystallization process are developed in the next section.

IV. EXTENSION OF SUPERCRITICAL FLUID ANTI-SOLVENT RECRYSTALLIZATION TO PRODUCTION SCALE OPERATION

A simplified process flow diagram for the recrystallization of RDX via the gas anti-solvent process is given in Figure 32. In explanation of its operation (and with reference to the accented flow path in the figure) RDX is charged to a dissolver (and it can be charged by means of a screw conveyor, for example), and a solvent (cyclohexanone, for example) is admitted in the appropriate ratio to dissolve the RDX. The pump, P-1, takes the RDX-cyclohexanone solution from ambient pressure to process pressure. Gas at process pressure is injected into the RDX-cyclohexanone solution via pump, P-4, the ratio of gas to solution set by the rates of the respective pumps. At the start of the sequence Valves 1 and 2 are open, 3 and 4 closed. The expanded solution is conveyed to the crystallizer, vessel 1, which is designed to provide sufficient residence time to produce 100 micron RDX. The filter element serves to retain the RDX and allows the expanded liquid (cyclohexanone and gas) to pass through. The solution passes through V-2, and is expanded slightly through the pressure reduction valve, PRV, where the solution separates in organic liquid and gas. The gas is liquefied and pumped by P-2 to an in-process storage vessel. Solvent is recycled to the dissolver.

When the designed-for amount of RDX has been collected, Valves 3 and 4 are opened, Valves 1 and 2 closed, the expanded solution leaving pump, P-1, is conveyed to Crystallizer 2, and the process of recrystallization continued as just described. While recrystallization is continuing in Vessel 2, the RDX crystals in Vessel 1 are washed off their adhering solvent with fresh liquefied gas via pump, P-5, through valve, V-5.

Many "details" of operation and design are being ignored for this preliminary flow sheet and process description, but the "details", of course, influence economics, ease of operation, and the like. One method of removing the crystals from the vessel, for example, might be via a "basket" insert in the crystallizer. The basket might be a very thin walled cylinder fitted with a sintered metal element at the base, the entire basket placed into the vessel so as to prevent bypassing of expanded solution and RDX particles. A quick opening autoclave top on the vessel would provide access to the interior for inserting an empty basket and removing a filled one.

Irrespective of the design details, in any event, at the end of the respective recrystallization and washing segments the flow of expanded solution is again interchanged and the process continued as previously. The advantage of the dual recrystallizer system is that the down-time is minimized, for example, if crystallizer 2 was not included in the design, the crystal washing step, unloading, and insertion of a new basket would be carried out during down-time, i.e., no production occurring.

It is felt that the two crystallizer vessel system is a reasonable one for this preliminary cost evaluation; the methodology for developing the capital and operating costs follows.

FIGURE 32 - SUPERCRITICAL FLUID ANTI-SOLVENT PRECIPITATION

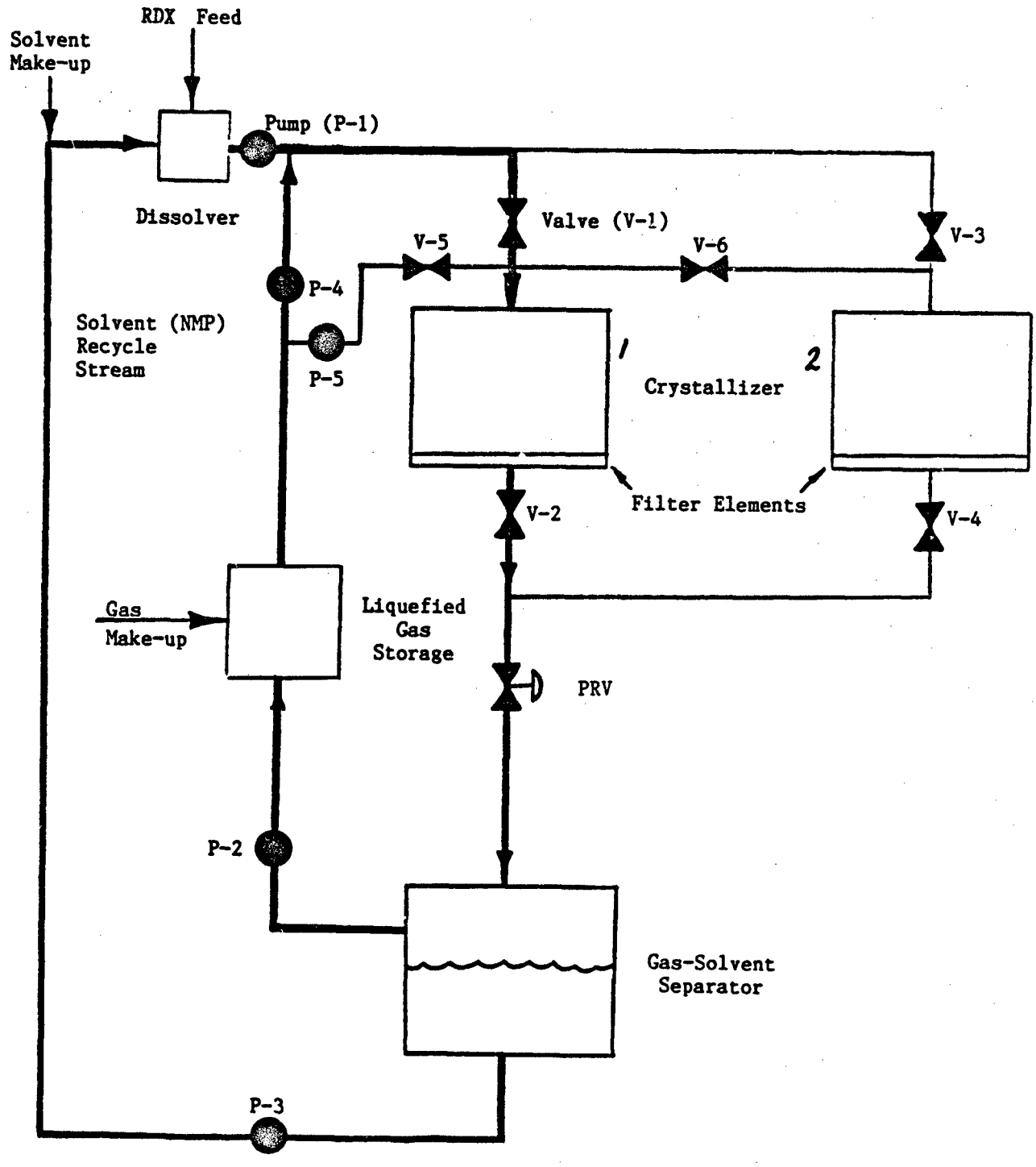

Basis

a. Production level: 10,000,000 lbs/yr

b. Solubility level of RDX in cyclohexanone: 10%

c. Anti-solvent: carbon dioxide

d. Pressure level: 800 psig max.

e. Cycle time: 1 hr
(Cycle time influences vessel size and cost)

f. Work schedule: 3 shifts/day, 330 days/yr

The 10,000,000 lb - 330 day production schedule calculates to 30,303 lbs/day which on a Chemical Process Industries standard is not a huge volume of material. Production figures are relatively lower, and the 30,000 lb/day production rate is more related to one for fine chemicals, which RDX can be considered to be. During the 1 hr cycle time about 1200 lbs of RDX are recrystallized and collected in the basket; a 1200 lb load plus, say, 200 or 300 lbs for the basket is a tractable load for a simple block and tackle or light weight overhead crane system to handle; assuming a bulk density of about 0.8 to 1 g/cc the minimum volume of the basket would be about 20 ft^3; for a more conservative design it is doubled to 40 ft^3. For a comparison, the vessels that are used for coffee decaffeination (at the Hag plant in Bremen, FRG) are 1000(!) ft^3 in volume and hold 40,000 lbs of coffee beans per fill. Furthermore, those vessels operate at 5000 psi whereas RDX recrystallization operates at only 150 psi. As further comparison of processes the volume of organic solution that is pumped from the dissolver (by Pump, P-1) is only 25 gpm; a "few" horsepower motor is more than sufficient to provide a 150 psi head. For the coffee plant the solvent recirculation pump is 5000 Hp (and it is for the ability to provide these comparisons that the background and applications of supercritical fluids was given in some detail in Section II).

Phasex Corporation formed an association with the Glitsch Package Plants Division in 1986; during the last year and one-half three skid mounted supercritical fluid plants have been designed and construction of one of them is almost completed. The cost for small plants, of the order of a few million lbs/yr, is, therefore, reasonably well known. Figure 33 is a very detailed piping and instrumentation diagram (P/ID) for one of the plants. The "nuts and bolts" design or even the detail required for the P/ID was outside the scope of the Phase I program; however, based upon the similarities between the RDX recrystallization process and the other processes the cost of the 10,000,000 lbs/yr recrystallization plant is estimated at about $5.0MM.

In order to arrive at a recrystallization cost, then, bases a-f, a plant cost of $5.0MM, and the following additional conditions are stipulated:

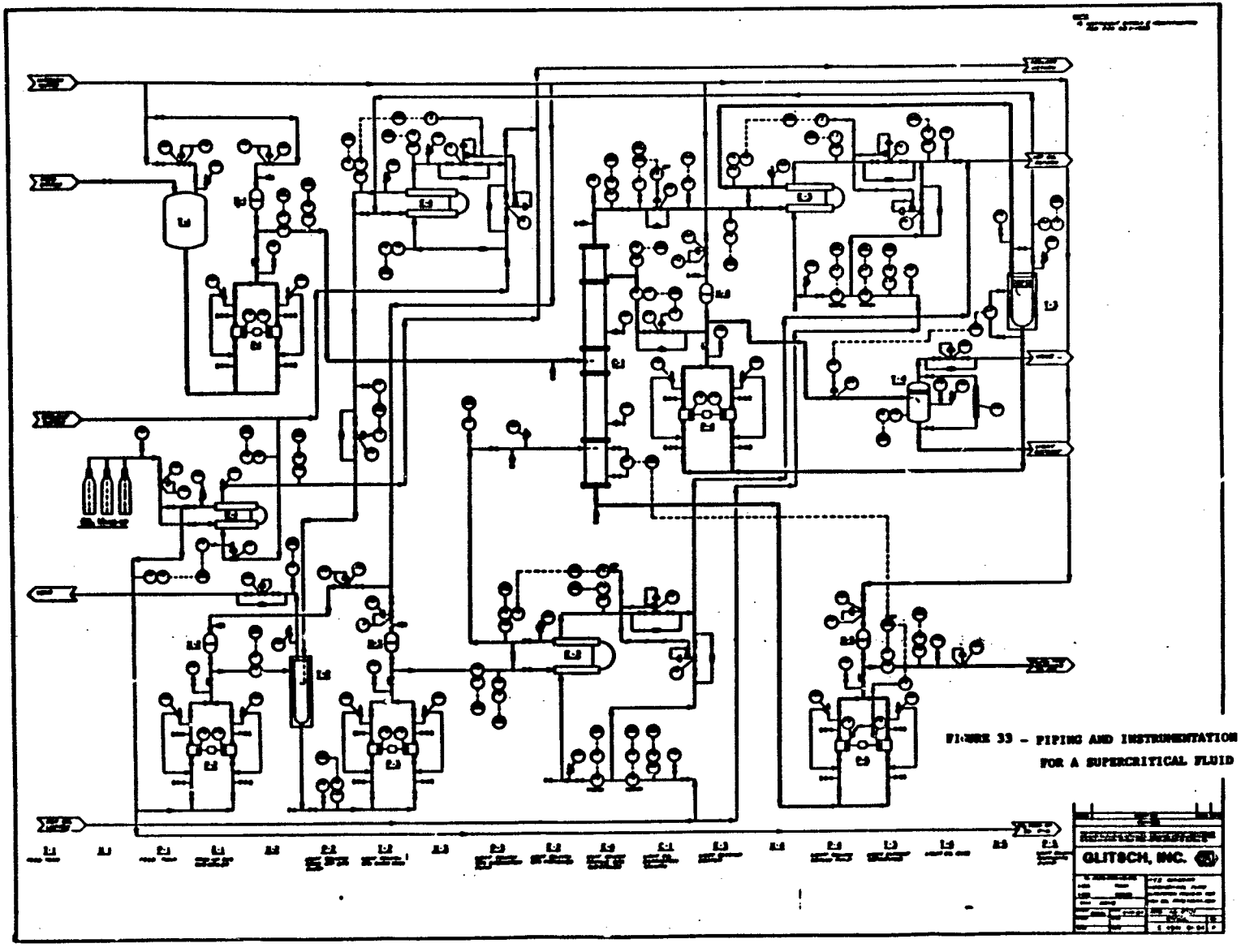

FIGURE 33 – PIPING AND INSTRUMENTATION DIAGRAM (P/ID) FOR A SUPERCRITICAL FLUID PLANT

1. 4 persons/shift = 3,960 person days/yr

2. Salary plus fringes assumed to be $150/person day;
   Labor costs = 3,960 x 150/10MM = 36¢/lb

3. Depreciation schedule, 5 yr straight line;
   Capital costs = $5MM/(10MM lbs x 5 yrs) = 10¢/lb

4. Buildings, facilities, 20% of capital costs = 2¢/lb

5. Maintenance, 10% of capital costs = 1.2¢/lb

6. Insurance, taxes, 10% of capital costs = 1.2¢/lb

7. Supervision, materials flow accounting for transfer costs, 100% of labor costs = 6¢/lb

8. Gas and solvent make-up, utilities; no gas and solvent make-up values were evaluated on Phase I but for conservatism a high cost will be estimated, viz., 20¢/lb

Table III summarizes the costs.

Table III

Capital and Operating Costs for Gas Anti-Solvent Recrystallization of RDX (10,000,000 lbs/yr)

Capital Costs	
Plant and buildings	12¢/lb
Operating Costs	
Labor	6
Maintenance	1.2
Insurance, Taxes	1.2
Supervision, Accounting	6
Make-up, Utilities	20
Total Costs	47¢/lb

Since this estimate is of a preliminary nature, it is suggested that a cost range of about $0.50 to $1.00/lb RDX be considered as the capital and operating cost for recrystallizing RDX.

V. CONCLUSIONS AND RECOMMENDATIONS

A. Conclusions

1. Recrystallization of RDX by Supercritical Fluid Anti-Solvents has been demonstrated to be an effective technique to form RDX free of intragranular cavities.

2. With appropriate combinations of parameters particle size can be controlled; RDX crystals of quite narrow particle size distribution could be formed ranging in average particle size from about 10 microns to about 100 microns. The 10 micron size RDX is very difficult to produce by the conventional Holsten AAP process.

3. A preliminary economic analysis showed that at a processing level of 10,000,000 lbs/yr of RDX, the supercritical fluid anti-solvent process could recrystallize RDX at total capital and operating costs of about $0.50 to $1.00/lb.

4. Other capabilities of the supercritical fluid anti-solvent process were suggested, viz., co-precipitation of explosives and other materials and the coating of explosive crystals with polymers.

B. Recommendations

1. Because of the positive results obtained on the Phase I program, a Phase II study should be carried out.

2. The other processing potentials of supercritical fluid anti-solvents described should be evaluated at the feasibility level.

VI. LITERATURE CITATIONS

1. Booth, H.S. and R.M. Bidwell, Solubility Measurements in the Critical Region, Chem. Rev., 44, 477-513 (1949).

2. Paul, P.M.F. and W S. Wise, The Principles of Gas Extraction, Mills and Boon LTD, London, 1971.

3. Irani, C.A. and E.W. Funk, Separation Using Supercritical Gases, in CRC Handbook: Recent Developments in Separation Science, Vol. III, Part A, CRC Press, Boca Raton, FL, 171-179 (1977).

4. Paulaitis, M.E., V.J. Krukonis, R.T. Kurnik, and R.C. Reid, Supercritical Fluid Extraction, Rev. in Chem. Eng., 1(2), 179-250 (1983).

5. Diepen, G.A.M. and F.E.C. Scheffer, On Critical Phenomena of Saturated Solutions in Binary Systems, J. Am. Chem. Soc., 4081-5 (1948).

6. Diepen, G.A.M. and F.E.C. Scheffer, The Solubility of Naphthalene in Supercritical Ethylene, J. Am. Chem. Soc., 70, 4085-9 (1948).

7. Diepen, G.A.M. and F.E.C. Scheffer, The Solubility of Naphthalene in Supercritical Ethylene II, J. Phys. Chem., 57, 575-8 (1953).

8. MacKay, M.E. and M.E. Paulaitis, Solid Solubilities of Heavy Hydrocarbons in Supercritical Solvents, Ind. Eng. Chem. Fund., 18, 144-53 (1979).

9. McHugh, M.A. and M.E. Paulaitis, Solid Solubilities of Naphthalene and Biphenyl in Supercritical Carbon Dioxide, J. Chem. Eng. Data, 25, 326-9 (1980).

10. Kurnik, R.T. and R.C. Reid, Solubility of Solid Mixtures in Supercritical Fluids, Fluid Phase Equilibria, 8, 93-105 (1982).

11. Hannay, J.B. and J. Hogarth, On the Solubility of Solids in Gases, Proc. Roy. Soc., (London), 29, 324-26 (1879).

12. Tsekhanskaya, Yu.V., M.B. Iomtev, and E.V. Mushkina, Solubility of Diphenylamine and Naphthalene in Ethylene and Carbon Dioxide Under Pressure, Russ., J. Phys. Chem., 36, 1177-81 (1962).

13. Tsekhanskaya, Yu.V., M.B. Iomtev, and E.V. Mushkina, Solubility of Naphthalene in Ethylene and Carbon Dioxide Under Pressure, Russ. J. Phys. Chem., 38, 1173-6 (1964).

14. Tsekhanskaya, Yu.V., Diffusion of Naphthalene in Carbon Dioxide Near Liquid-Gas Critical Point, Russ. J. Phys. Chem., 45, 744-44 (1971).

15. King, A.D., and W.W. Robertson, Solubility of Naphthalene in Compressed Gases, J. Chem. Phys., 37, 1453-5 (1962).

16. Najour, G.C. and A.D. King, Jr., Solubility of Naphthalene in Compressed Methane, Ethylene and Carbon Dioxide, J. Chem. Phys., 45, 1915-21 (1966).

17. Schmitt, W.J. and R.C. Reid, Solubilities of Several Model Organic Compounds in Chemically Different Supercritical Fluids, Annual Meeting, AIChE, San Francisco, November 1984.

18. Krukonis, V.J., M.A. McHugh, A.J. Seckner, Xenon as a Supercritical Solvent, J. Phys. Chem., 88, 2687-9 (1984).

19. McHugh, M.A., A.J. Seckner, and V.J. Krukonis, Supercritical Xenon, Annual Meeting, AIChE, San Francisco, November 1984.

20. McHugh, M.A., A.J. Seckner, and T.J. Yogan, High Pressure Phase Behavior of Mixtures of Carbon Dioxide and Octacosane, IEC Fundamentals, 23, 493-496 (1984).

21. Najour, G.C. and A.D. King, Jr., Solubility of Anthracene in Compressed Methane, Ethylene, and Carbon Dioxide: The Correlation of Anthracene-gas Second Virial Coefficients Using Pseudocritical Parameters, J. Chem. Phys., 52, 5206-11 (1970).

22. Eisenbeiss, J., A Basic Study of the Solubility of Solids in Gases at High Pressures, Final Report, Contract No. DA18-108-AMC-244(A), Southwest Research Inst., San Antonio, (August 6, 1964).

23. Kurnik, R.T., S.J. Holla, and R.C. Reid, Solubility of Solids in Supercritical Carbon Dioxide and Ethylene, J. Chem. Eng. Data, 26, 47-51 (1981).

24. Kennedy, G.C., A Portion of the System Silica-Water, Econ, Geol., 45, 629-36 (1950).

25. VanLeer, R.A. and M.E. Paulaitis, Solubilities of Phenol and Chlorinated Phenols in Supercritical Carbon Dioxide, J. Chem. Eng. Data, 25, 257-9 (1980).

26. Holden, C.H. and O. Maass, Solubility Measurement in the Region of the Critical Point, Can. J. Res. 18B, 293-304 (1940).

27. Ewald, A.H., The Solubility of Solids in Gases, Trans. Far. Socl, 49, 1401-85 (1953).

29. Todd, D.B., and J.C. Elgin, Phase Equilibria in Systems with Ethylene Above Its Critical Temperature, AIChE J., 1, 20-7 (1955).

30. Caragay, A.B., Supercritical Fluids for Extraction of Flavors and Fragrances from Natural Products, Perf. and Flavors, 6, 43-55 (1981).

31. Schultz, W.G., J.N. Randal, Liquid Carbon Dioxide for Selective Aroma Extraction, Food Tech., 24, 94-8 (1970).

32. Randall, J.M., W.G. Schultz, A.I. Morgan, Jr., Extraction of Fruit Juices and Concentrated Essences with Liquid Carbon Dioxide, Confructa, 16, 10-16 (1971).

33. Anon., A Supercritical Fluid Extraction Alternative to Distillation of Alcohol, Chem. Eng., 88(9), 19 (1981).

34. Paulaitis, M.E., M.L. Gilbert, and C.A. Nash, Separation of Ethanol-Water Mixtures with Supercritical Fluids, 2nd World Congress of Chemical Engineering, Montreal, October 1981.

35. Moses, J.M., K.E. Goklen, and R.P. deFilippi, Pilot Plant Critical-Fluid Extraction of Organics from Water, Annual Meeting, AIChE, Los Angeles, November 1982.

36. McHugh, M.A., M.W. Mallet, and J.P. Kohn, High Pressure Phase Equilibria of Alcohol-Water-Supercritical Solvent Mixtures, Annual Meeting, AIChE, New Orleans, November 1981.

37. Modell, M., R.P. deFilippi, and V.J. Krukonis, Regeneration of Activated Carbon with Supercritical Carbon Dioxide, Amer. Chem. Soc. Meeting, Miami, September 1978.

38. Modell, M., R.J. Robey, V.J. Krukonis, and R.P. deFilippi, Supercritical Fluid Regeneration of Activated Carbon, 87th National Meeting, AIChE, Boston, August 1979.

39. Zosel, K., Separation with Supercritical Gases: Practical Applications, Angew. Chem. Int. Ed. Engl., 17, 702-15 (1978).

40. Roseluis, W., O. Vitzthum, and P. Hubert, Method for the Production of Caffeine-Free Coffee Extract, U.S. Patent 3,843,824; 22 October 1974.

41. Prasad, R., M. Gottesman, and R.A. Scarella, Decaffeination of Aqueous Extracts, U.S. Patent 4,246,291; 20 January 1981.

42. Margolis, G. and J. Chiovini, Decaffeination Process, U.S. Patent 4,251,559; 17 February 1981.

43. Friedrich, J.P., G.R. List, and A.J. Leakin, Petroleum - Free Extraction of Oil from Soybeans with Supercritical CO_2, J. Amer. Oil Chem. Soc., 59(7), 288-92 (1982).

44. Christianson, D.D., J.P. Friedrich, G.R. List, K. Warner, E.B. Bagley, A.C. Stringfellow, and G.E. Inglett, Supercritical Fluid Extraction of Dry-Milled Corn Germ with Carbon Dioxide, J. Food Sci., 49(1) 229-32 and 272 (1984).

45. Stahl, E., E. Shutz, and H.K. Mangold, Extraction of Seed Oils with Liquid and Supercritical Carbon Dioxide, Ag. Food Chem., 28, 1153-7 (1980).

46. Anon., Extraction Process Benefits Potato Chips, Coffee, Hops, Food Eng. Int., 45-6, October 1981.

47. Wise, W.S., Solvent Extraction of Coal, Chem. Ind., (London), 950-1 (1970).

48. Gearhart, J.A. and L. Garwin, Resid-Extraction Process Offers Flexibility, Oil Gas J., 74(24), 63-6 (1976).

49. Gangoli, N. and G. Thodas, Liquid Fuels and Chemical Feedstocks from Coal by Supercritical Gas Extraction, IEC, Prod. Res. Dev., 16(3), 208-16 (1977).

50. Stahl, E., W. Schilz, E. Schutz, and E. Willing, A Quick Method for the Microanalytical Evaluation of the Dissolving Power of Supercritical Gases, Angew. Chem. Int. Ed. Engl., 17, 731-8 (1978).

51. Krukonis, V.J., A.R. Branfman, and M.G. Broome, Supercritical Fluid Extraction of Plant Materials Containing Chemotherapeutic Drugs, 87th AIChE National Meeting, Boston, August 1979.

52. Fremont, H.A., Extraction of Coniferous Woods with Fluid Carbon Dioxide and Other Supercritical Fluids, U.S. Patent 4,308,200; 20 December 1981.

53. Anon., Gas Solvents: About to Blast Off, Bus. Week, July 27, 68M (1981).

54. Cookson, C.B., Subcritical Extractions Using Liquid CO_2, Spring Tech. Symp. Bulk Pharma. Chemicals, Newport, RI, May 1987.

55. Perkins, B., Food Without Cholesterol Close to Reality, The Cincinnati Enquirer, Jan. 10, D1 (1987).

56. Wilke, G., Studiengesellschaft Kohle, Mulkeim (Ruhr), W. Germany, private communication.

57. Krukonis, V.J., Processing of Polymers with Supercritical Fluids, Polymer News, 11, 7-16 (1985).

58. Krukonis, V.J., Supercritical Fluid Fractionation: An Alternative to Molecular Distillation, Nat. Mtg. AIChE, Houston, March 1983.

59. McHugh, M.A. and V.J. Krukonis, Supercritical Fluid Extraction: Principles and Practice, Ch.9, Butterworth Publishers, Boston (1986).

60a. Worthy, W., Supercritical Fluids Offer Improved Separations, C&E News, Aug. 3, 16-17 (1981).

60b. Paulaitis, M.E., V.J. Krukonis, R.T. Kurnik, and R.C. Reid, Supercritical Fluid Extraction, Rev. Chem. Eng. 1(2), 179-250 (1983).

60c. Krukonis, V.J., Supercritical Fluid Nucleation of Difficult-to-Comminute Solids, Ann. Mtg. AIChE, San Francisco, November 1984.

61. Larson, K.A. and M.L. King, Evaluation of Supercritical Fluid Extraction in the Pharmaceutical Industry, Biotech. Prog., 2, 73-82 (1986).

62. Petersen, R.C., D.W. Matson, and R.D. Smith, Precipitation of Polymeric Materials from Supercritical Fluid Solution, Polymer Prepr., 27, 261-62 (1987).

63. Elgin, J.C., and J.J. Weinstock, Phase Equilibria at Elevated Pressures in Ternary Systems of Ethylene and Water with Organic Liquids: Salting Out with a Supercritical Gas, J. Chem. Eng. Data 4, 3-10 (1959).

64. Paulaitis, M.E., J.R. DiAndreth, and R.G. Kander, An Experimental Study of Phase Equilibria for Isopropanol-Water-CO_2 Mixtures Related to Supercritical Fluid Extraction of Organic Compounds from Aqueous Solutions, in Supercritical Fluid Technology, J.M.L. Penninger, M. Radosz, M.A. McHugh, and V.J. Krukonis, eds., Elsevier Science Publishers, Amsterdam (1985).

65. Irani, C.A., C. Cosewith, and S.S. Kasegrande, New Methods for High Temperature Phase Separation of Solutions Containing Copolymer Elastomers, U.S. Patent 4,319,021 (1977).

66. McHugh, M.A. and T.L. Guckes, Separating Polymer Solutions with Supercritical Fluids, Macromolecules 18, 674-81 (1985).

67. Gibbs, J.W., The Collected Works of J.W. Gibbs, Vol. I Thermodynamics, p. 322, Yale University Press, New Haven, CT (1957).

68. Adamson, A.W., Physical Chemistry of Surfaces, pp. 288-298, Interscience Publishers, Easton, PA (1963).

DISTRIBUTION LIST

No of Copies	Organization
12	Administrator Defense Technical Info Center ATTN: DTIC-DDA Cameron Station Alexandria, VA 22304-6145
1	HQDA (SARD-TR) Washington, DC 20310-0001
1	Commander US Army Materiel Command ATTN: AMCDRA-ST 5001 Eisenhower Avenue Alexandria, VA 22333-0001
1	Commander US Army Laboratory Command ATTN: AMSLC-DL Adelphi, MD 20783-1145
2	Commander Armament RD&E Center US Army AMCCOM ATTN: SMCAR-MSI Picatinny Arsenal, NJ 07806-5000
2	Commander Armament RD&E Center US Army AMCCOM ATTN: SMCAR-TDC Picatinny Arsenal, NJ 07806-5000
1	Director Benet Weapons Laboratory Armament RD&E Center US Army AMCCOM ATTN: SMCAR-LCB-TL Watervliet, NY 12189-4050
1	Commander US Army Armament, Munitions and Chemical Command ATTN: SMCAR-ESP-L Rock Island, IL 61299-5000
1	Commander US Army Aviation Systems Command ATTN: AMSAV-DACL 4300 Goodfellow Blvd. St. Louis, MO 63120-1798
1	Director US Army Aviation Research and Technology Activity Ames Research Center Moffett Field, CA 94035-1099

No of Copies	Organization
1	Commander US Army Missile Command ATTN: AMSMI-AS Redstone Arsenal, AL 35898-5010
1	Commander US Army Tank Automotive Command ATTN: AMSTA-DDL (Technical Library) Warren, MI 48397-5000
1	Director US Army TRADOC Analysis Command ATTN: ATAA-SL White Sands Missile Range, NM 88002-5502
1	Commandant US Army Infantry School ATTN: ATSH-CD-CSO-OR Fort Benning, GA 31905-5660
1	AFWL/SUL Kirtland AFB, NM 87117-5800
1	Air Force Armament Laboratory ATTN: AFATL/DLODL Eglin AFB, FL 32542-5000
1	Chairman DOD Explosives Safety Board Room 856-C Hoffman Bldg 1 2461 Eisenhower Avenue Alexandria, VA 22331
1	Commander US Army Armament RD&E Center ATTN: SMCAR-LCE, Dr. N. Slagg Picatinny Arsenal, NJ 07806-5000
1	Commander US Army Armament, Munitions & Chemical Command ATTN: AMSMC-IMP-L Rock Island, IL 61299-7300

DISTRIBUTION LIST

No of Copies	Organization
1	Commander Belvoir RD&E Center ATTN: STRBE-JMC, Mr. Rick Martinez Fort Belvoir, VA 22060-5606
1	Commander US Army Aviation Systems Command ATTN: AMSAV-ES 4300 Goodfellow Boulevard St. Louis, MO 63120-1798
1	Commander CECOM R&D Technical Library ATTN: AMSEL-IM-L (Reports Section) B. 2700 Fort Monmouth, NJ 07703-5000
1	Director Missile and Space Intelligence Center ATTN: AIAMS-YDL Redstone Arsenal, AL 35898-5500
1	Commander US Army Missile Command ATTN: AMSME-RK, Dr. R.G. Rhoades Redstone Arsenal, AL 35898
1	Commandant USAOMMCS ATTN: ATSK-CME, S. Herman Redstone Arsenal, AL 35897-6500
1	Commander US Army Missile Command ATTN: AMSMI-RO-PR-T Dr. Porter Mitchell Redstone Arsenal, AL 35898
1	Commander US Army Development & Employment Agency ATTN: MODE-ORO Fort Lewis, WA 98433-5000
2	Commander US Army Research Office ATTN: Chemistry Division P.O. Box 12211 Research Triangle Park, NC 27709-2211
2	Office of Naval Research ATTN: Dr. A. Faulstich, Code 23 800 N. Quincy Street Arlington, VA 22217
1	Commander Naval Sea Systems Command ATTN: Dr. R. Bowen SEA 06I Washington, DC 20362
1	Commander Naval Explosive Ordnance Disposal Technology Center ATTN: Technical Library Code 604 Indian Head, MD 20640
1	Commander Naval Research Lab ATTN: Code 6100 Washington, DC 20375
1	Commander Naval Surface Weapons Center ATTN: Code G13 Dahlgren, VA 22448-5000
1	Commander Naval Surface Weapons Center ATTN: Mr. L. Roslund, R10C Silver Spring, MD 20903-5000
1	Commander Naval Surface Weapons Center ATTN: Mr. M. Stosz, R101 Silver Spring, MD 20903-5000
1	Commander Naval Surface Weapons Center ATTN: C. Gotzmer, R11 Indian Head, MD 20640-5000
1	Commander Naval Surface Weapons Center ATTN: Dr. R.C. Gill, Bldg 600 Indian Head, MD 20640-5000
1	Commander Naval Surface Weapons Center ATTN: Code X211, Lib Silver Spring, MD 20903-5000
1	Commander Naval Surface Weapons Center ATTN: R.R. Bernecker, R13 Silver Spring, MD 20903-5000
1	Commander Naval Surface Weapons Center ATTN: J.W. Forbes, R13 Silver Spring, MD 20903-5000

DISTRIBUTION LIST

No of Copies	Organization
1	Commander Naval Surface Weapons Center ATTN: S. J. Jacobs, R10 Silver Spring, MD 20903-5000
1	Commander Naval Surface Weapons Center ATTN: J. Short, R12 Silver Spring, MD 20903-5000
1	Commander Naval Weapons Center ATTN: L. H. Josephson, Code 326B China Lake, CA 93555
1	Commander Naval Weapons Center ATTN: M. Chan, Code 3891 China Lake, CA 93555
1	Commander Naval Weapons Center ATTN: Dr. B. Lee, Code 3264 China Lake, CA 93555
1	Commander Naval Weapons Center ATTN: Dr. L. Smith, Code 326 China Lake, CA 93555
1	Commander Naval Weapons Center ATTN: Dr. R. Atkins, Code 385 China Lake, CA 93555
1	Commander Naval Weapons Center ATTN: Dr. R. Reed, Code 388 China Lake, CA 93555
1	Commander Naval Weapons Center ATTN: Dr. K.J. Graham, Code 3891 China Lake, CA 93555-6001
1	Commander Naval Weapons Station NEDED ATTN: Dr. Louis Rothstein, Code 50 Yorktown, VA 23691
1	Commander Fleet Marine Force, Atlantic ATTN: G-4 (NSAP) Norfolk, VA 23511
1	Commander Air Force Rocket Propulsion Laboratory ATTN: Mr. R. Geisler, Code AFRPL MKPA Edwards AFB, CA 93523
3	AFATL/MNE ATTN: G. Parsons M. Patrick Eglin AFB, FL 32542-5000
1	Commander Ballistic Missile Defense Advanced Technology Center ATTN: Dr. David C. Sayles P.O. Box 1500 Huntsville, AL 35807
1	Director Lawrence Livermore National Laboratory University of California ATTN: Dr. M. Finger P.O. Box 808 Livermore, CA 94550
1	Director Lawrence Livermore National Laboratory University of California ATTN: Dr. R. McGuire P.O. Box 808 Livermore, CA 94550
1	Director Los Alamos National Laboratory ATTN: Mr. J. Ramsey P.O. Box 1663 Los Alamos, NM 87545
1	Director Los Alamos National Laboratory ATTN: Dr. L. Stretz P.O. Box 1663 Los Alamos, NM 87545
1	Sandia National Laboratories ATTN: Dr. E. Mitchell, Supervisor Division 2513 P.O. Box 5800 Albuquerque, NM 87185
10	Central Intelligence Agency OIR/DB/Standard GE47 HQ Washington, DC 20505

DISTRIBUTION LIST

No of
Copies Organization

1 Irving B. Akst
IDOS Corporation
P.O. Box 285
Pampa, TX 79065

1 Holston Defense Corporation
ATTN: D.M. Mahaffey, Superintendent
Kingsport, TN 37660

Aberdeen Proving Ground
Dir, USAMSAA
ATTN: AMXSY-D
AMXSY-MP, H. Cohen
Cdr, USATECOM
ATTN: AMSTE-TO-F
AMSTE-SI-F
Cdr, CRDEC, AMCCOM
ATTN: SMCCR-RSP-A
SMCCR-MU
SMCCR-SPS-IL
SMCCR-OPP, C. Hassell

END

6-89

DTIC